Electronic Structure of 2,2′-Bipyridine Organotransition-Metal Complexes. Establishing the Ligand Oxidation Level by Density Functional Theoretical Calculations

Christopher C. Scarborough and Karl Wieghardt*

Max-Planck-Institut für Bioanorganische Chemie, Stiftstrasse 34-36, D-45470 Mülheim an der Ruhr, Germany

Ⓢ Supporting Information

ABSTRACT: A density functional theoretical (DFT) study (B3LYP) has been carried out on 20 organometallic complexes containing η^5- and/or η^3-coordinated cyclopentadienyl anions (Cp^-) and 2,2′-bipyridine (bpy) ligand(s) at varying oxidation levels, i.e., as the neutral ligand (bpy^0), as the π-radical monoanion $(bpy^{\bullet-})^-$, or as the diamagnetic dianion $(bpy^{2-})^{2-}$. The molecular and electronic structures of these species in their ground states and, in some cases, their first excited states have been calculated using broken-symmetry methodology. The results are compared with experimental structural and spectroscopic data (where available) in order to validate the DFT computational approach. The following electron-transfer series and complexes have been studied: $[(Cp)_2V(bpy)]^{0,+,2+}$ (**1−3**), $[(Cp)_2Ti(bpy)]^{-,0,+,2+}$ (**4−7**), $[(Cp)_2Ti(biquinoline)]^{0,+}$ (**8 and 9**), $[(Cp^*)_2Ti(bpy)]^0$ (**10**) (Cp^* = pentamethylcyclopentadienyl anion), $[Cp^*Co(bpy)]^{0,+}$ (**11 and 12**), $[Cp^*Co(bpy)Cl]^{+,0}$ (**13 and 14**), $[Fe(toluene)(bpy)]^0$ (**15**), $[Cp^*Ru(bpy)]^-$ (**16**), $[(Cp)_2Zr(bpy)]^0$ (**17**), and $[Mn(CO)_3(bpy)]^-$ (**18**). In order to test the predictive power of our computations, we have also calculated the molecular and electronic structures of two complexes, **A** and **B**, namely, the diamagnetic dimer $[Cp^*Sc(bpy)(\mu\text{-}Cl)]_2$ (**A**) and the paramagnetic (at 25 °C) mononuclear species $[(\eta^5\text{-}C_5H_4(CH_2)_2N(CH_3)_2)Sc(^mbpy)_2]$ (**B**). The crystallographically observed intramolecular $\pi-\pi$ interaction of two N,N′-coordinated π-radical anions in **A** leading to an $S = 0$ ground state is reliably reproduced. Similarly, the small singlet−triplet gap of ∼600 cm^{-1} between two antiferromagnetically coupled $(bpy^{\bullet-})^-$ ligands in **B**, two ferromagnetically coupled radical anions in the triplet excited state of **B**, and the structures of **A** and **B** is reproduced. Therefore, we are confident that we can present computationally obtained, detailed electronic structures for complexes **1−18**. We show that N,N′-coordinated neutral bpy^0 ligands behave as very weak π acceptors (if at all), whereas the $(bpy^{2-})^{2-}$ dianions are strong π-donor ligands.
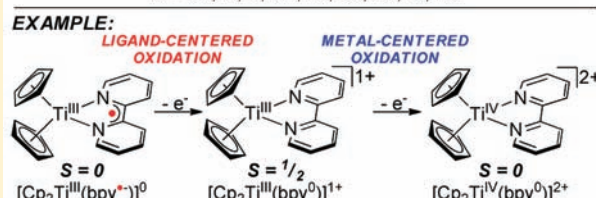
■ INTRODUCTION

2,2′-Bipyridine (bpy) and its C-substituted derivatives are arguably the most commonly used bidentate nitrogen-donor ligands in coordination chemistry.[1] Many main-group metal ions, lanthanoid ions, actinoid ions, and transition-metal ions form coordination compounds containing up to four N,N′-coordinated ligands.[2] It was recognized very early that these bpy ligands[2] can exist in three different oxidation levels, all of which have been characterized by X-ray crystallography. These are the neutral (bpy^0),[3] the π-radical monoanion $[(bpy^{\bullet-})^-]$,[4] and the diamagnetic dianion $[(bpy^{2-})^{2-}]$[5] (Figure 1 and Table 1). All of these forms can bind in a bidentate fashion to a Lewis acid such as a main-group metal ion like Al^{III},[6,7] a transition-metal ion,[8,9] and lanthanoid[10] or actinoid[11] ions. The structures of some transition-metal-ion, lanthanoid, and actinoid complexes containing the π-radical monoanion $(bpy^{\bullet-})^-$ are given in refs 8−10 and 11, respectively. The problem is, how do we determine the ligand oxidation level in a given coordination compound unambiguously? A very clear example for the observed structural changes between N,N′-coordinated bpy^0 and dianion $(bpy^{2-})^{2-}$ is shown in Figure 1 for the two diamagnetic

complexes $[Al^{III}Cl_2(bpy^0)_2]Cl \cdot MeCN$[6] and $[Li(THF)_4][Al^{III}\text{-}(bpy^{2-})_2]$ (THF = tetrahydrofuran).[7] The characteristic structural features of an uncoordinated neutral[3] (bpy^0) and alkaline salts of the monoanion[4] $(bpy^{\bullet-})^-$ and dianion[5] $(bpy^{2-})^{2-}$ are summarized in Table 1.

The lowest unoccupied molecular orbital (LUMO) of neutral bpy^0 shown in Figure 1c is π bonding between C1−C1′ and C2−C3 and π antibonding between C1−N, C1−C2, and C3−C4. It is therefore expected that filling of this LUMO with one or two electrons will result in a stepwise shortening of the C1−C1′ and C2−C3 bonds in the π-radical monoanion and the diamagnetic dianion, respectively, whereas the bonds C1−N, C1−C2, and C3−C4 are expected to undergo some expansion (Table 1). Experimentally, the bond C1−C1′ exhibits the largest structural change upon one- and two-electron reduction: $bpy^0 \rightarrow (bpy^{\bullet-})^- \rightarrow (bpy^{2-})^{2-}$: ∼1.49 Å → ∼1.43 Å → ∼1.38 Å.
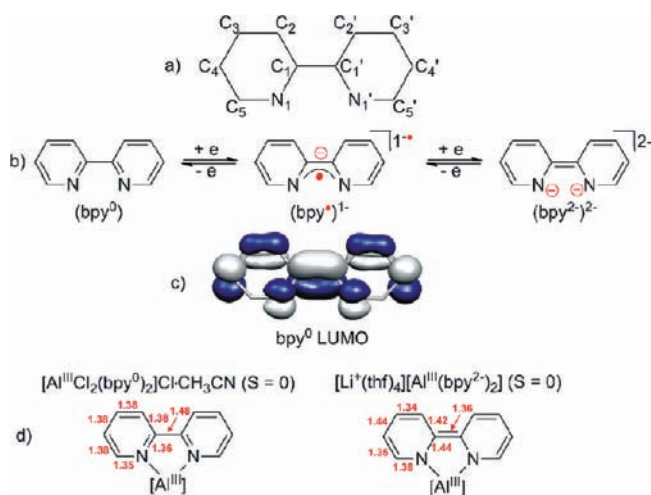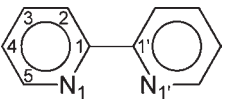
Figure 1. (a) Numbering scheme of the bpy ligand used in this work; (b) oxidation levels of bpy; (c) π^*-LUMO of bpy; (d) intraligand bond lengths of an $Al^{III}(bpy^0)$ complex (left, ref 6) and an $Al^{III}(bpy^{2-})$ complex (right, ref 7).

Table 1. Bond Lengths (Å) of the Neutral, Monoanionic, and Dianionic 2,2′-Bipyridine Ligands $[(bpy^0), (bpy^{\bullet-})^-$, and $(bpy^{2-})^{2-}]$

bond, Å	$(bpy^0)^3$	$(bpy^{\bullet-})^{-\,4a}$	$(bpy^{2-})^{2-\,5}$
C1—C1′	1.490(3)	1.431(3)	1.376(4)
C1—N1	1.346(2)	1.388(2), 1.391(3)	1.437(4), 1.436(5)
C5—N1	1.341(2)	1.337(2), 1.337(2)	1.336(4), 1.337(4)
C4—C5	1.384(2)	1.375(3), 1.372(3)	1.365(5), 1.365(6)
C3—C4	1.383(3)	1.403(3), 1.406(4)	1.410(6), 1.412(7)
C2—C3	1.385(2)	1.366(3), 1.363(3)	1.335(6), 1.336(6)
C1—C2	1.394(2)	1.429(3), 1.428(2)	1.447(5), 1.448(5)

It has been repeatedly stated in the literature that an a priori assignment of a bpy oxidation level (neutral, π-radical anion, and dianion) based solely on the intraligand bond lengths in a given transition-metal complex is not feasible "because a one-electron reduction of the $[(bpy^0)]$ ligand has the same qualitative effect as enhanced π-backbonding from a reduced metal center."[3,8] It is this notion that, in the past, has hampered the correct electronic structural description of a number of so-called "low-valent" organotransition-metal complexes containing reduced N,N′-coordinated bpy ligands (mono- or dianions).

In our view, the π-accepting character of neutral N,N′-coordinated bpy ligands and its influence on the C—C and C—N bond distances have been overestimated in the literature.[12-14] This was already pointed out by Tom Dieck et al. in 1975.[15] Neutral bpy^0 has been classified as a *weak π acceptor* in the spectrochemical series, and *no significant structural changes have been observed upon coordination to high- or low-valent transition-metal ions that could unambiguously be attributed to π-acceptor properties.* Consider, for example, the crystal structures of $[M^{II}(bpy^0)_3]^{2+}$ ($S = 0$), where M = Fe, Ru, and Os, each possess a filled t_{2g}^6 metal d-orbital set,[16] which is, in principle, ideally suited for the study of

metal-to-ligand π backdonation. Clearly, the C—N and C—C bond distances of these dications (Table 2) are indistinguishable within the 3σ error limits: specifically, the C1—C1′ bonds are invariably at 1.47 ± 0.01 Å. The same holds true for the trications $[(M^{III}(bpy^0)_3]^{3+}$ (M = Co, Rh, Ir), which also possess a t_{2g}^6 electron configuration.[17] The corresponding complexes $[Cr^{III}(bpy^0)_3]^{3+18}$ and $[Ga^{III}(bpy^0)_3]^{3+19}$ containing metal ions with $3d^3$ and $3d^{10}$ electron configurations, respectively, display the same metrical details of the bpy^0 ligands as the other species described above. Although we have found no *structural* evidence that bpy^0 is a π acceptor, the magnitude of the error in the bond lengths determined by X-ray crystallography is large enough that very *weak π-back-bonding interactions cannot be observed by this technique. UV—vis absorption spectroscopy is a much more sensitive tool to address the question of whether bpy^0 is a π acceptor, and such studies[20] have revealed that bpy^0 is indeed a *very* weak π acceptor (much weaker than CN^-), consistent with this effect being too small to observe crystallographically.

In this context, it is also interesting and revealing that the diamagnetic neutral complex $[(CO)_4Cr^0(bpy^0)]^0$, first prepared in 1935[21] and crystallographically characterized in 1992,[22] displays the same structural features of an undisturbed neutral bpy^0 ligand[3] [C1—C1′ at 1.471(5) Å] as in $[Cr^{III}(bpy^0)_3]^{3+}$.[18] This neutral complex has been chemically (Na) and electrochemically reduced by one electron, generating the paramagnetic monoanion $[(CO)_4Cr^0(bpy^{\bullet-})]^-$ ($S = {}^1/_2$);[23] the electron paramagnetic resonance (EPR) spectrum, the UV—vis spectrum, and its geometry-optimized-calculated (density functional theory, DFT) structure[24] unambiguously reveal the presence of an N,N′-coordinated radical monoanion $(bpy^{\bullet-})^-$ (the calculated C1—C1′ distance is short, at 1.423 Å). The neutral species has also been electrochemically one-electron-oxidized, affording the paramagnetic monocation $[(CO)_4Cr^I(bpy^0)]^+$ ($S = {}^1/_2$). Its EPR spectrum and calculated structure[25] unambiguously show that the central chromium ion possesses a low-spin d^5 ($S = {}^1/_2$) electron configuration and a *neutral* bpy^0 ligand. We note in passing that the above monoanion, prepared in 1972 by Kaizu and Kobayashi, is probably the first transition-metal-ion complex containing a $(bpy^{\bullet-})^-$ ligand that has been correctly identified as such.[23a,b]

It is noteworthy that all complexes containing a bona fide N,N′-coordinated $(bpy^{\bullet-})^-$ π-radical monoanion[8-11] display C1—C1′ bonds in the rather narrow range of 1.41—1.43 Å (Table 3). Again, there is no continuous variation of this bond with varying π-donor (or acceptor) strength of the central metal ion observed.

To the best of our knowledge, N,N′-coordinated $(bpy^{2-})^{2-}$ dianions have unambiguously been structurally characterized only three times, namely, in tetrahedral $[Al^{III}(bpy^{2-})_2]^-$, in $[Zr^{IV}(bpy^{2-})_3]^{2-}$, and in $[La^{III}(Tp^{Me2})(bpy^{2-})(THF)_2]^0$, in refs 7, 12, and 9, respectively. In all three cases, the C1—C1′ bond at 1.36 ± 0.01 Å is indicative of a C=C double bond. Thus, the three oxidation levels of N,N′-coordinated bpy ligands can, in principle, be readily identified by X-ray crystallography. For example, in a recent report, Irwin et al.[8] have reported the crystal structures of $[Fe^{II}(bpy^0)(mes)_2]^0$ and its one-electron-reduced monoanion $[Fe^{II}(bpy^{\bullet-})(mes)_2]^-$ (mes represents the ligand $2,4,6$-$Me_3C_6H_2^-$). The metrical details of bpy^0 and of its radical monoanion $(bpy^{\bullet-})^-$ clearly show that both forms can be identified and differentiated by X-ray crystallography (Table 3). The N,N′-coordinated π-radical anion exhibits a C1—C1′ bond length at 1.418(3) Å, whereas the same bond in the neutral bpy^0 ligand is found at 1.481(3) Å.

9774

dx.doi.org/10.1021/ic2005419 |*Inorg. Chem.* 2011, 50, 9773–9793

Table 2. Experimental Bond Lengths (Averaged) in N,N′-Coordinated Neutral bpy Ligands in $[M(bpy^0)_3]^{n+}$ Complexes (Numbering Scheme as in Table 1)

complex	ref	C1−C1′, Å	C1−N1, Å	C5−N1, Å	C4−C5, Å	C3−C4, Å	C2−C3, Å	C1−C2, Å
$[Cr^{III}(bpy^0)_3]^{3+}$	18	1.470(8)	1.348(9)	1.361(8)	1.357(10)	1.357(20)	1.380(10)	1.370(9)
$[Fe^{II}(bpy^0)_3]^{2+}$	16a	1.472(7)	1.350(5)	1.353(5)	1.379(5)	1.379(7)	1.385(5)	1.384(5)
$[Ru^{II}(bpy^0)_3]^{2+}$	16b	1.474(8)	1.354(6)	1.348(6)	1.374(6)	1.372(8)	1.388(8)	1.379(7)
$[Os^{II}(bpy^0)_3]^{2+}$	16c	1.495(7)	1.359(9)	1.349(7)	1.359(9)	1.38(1)	1.366(9)	1.388(8)
$[Co^{III}(bpy^0)_3]^{3+}$	17a	1.468(4)	1.360(4)	1.339(4)	1.374(4)	1.359(5)	1.371(5)	1.377(5)
$[Rh^{III}(bpy^0)_3]^{3+}$	17b	1.48(2)	1.34(2)	1.36(1)	1.36(2)	1.38(2)	1.37(2)	1.39(1)
$[Ir^{III}(bpy^0)_3]^{3+}$	17c	1.45(1)	1.36(2)	1.31(3)	1.39(3)	1.35(3)	1.35(3)	1.37(3)
$[Ga^{III}(bpy^0)_3]^{3+}$	19	1.478(9)	1.353(9)	1.340(9)	1.39(1)	1.37(1)	1.395(10)	1.38(1)
$[Zr^{IV}(bpy^{2-})_3]^{2-}$	12	1.360(9)	1.437(7)	1.370(9)	1.357(10)	1.44(1)	1.34(1)	1.433(9)

Table 3. Crystallographic Bond Lengths in N,N′-Coordinated bpy Ligands in Selected Complexes (Atom Numbering as in Table 1)

complex	ref	C1−C1′, Å	C1−N1, Å	C5−N1, Å	C4−C5, Å	C3−C4, Å	C2−C3, Å	C1−C2, Å
A	26	1.419(9), 1.415(9)	1.387(8), 1.397(8)	1.351(8), 1.346(8)	1.370(8), 1.373(7)	1.403(7), 1.411(7)	1.367(9), 1.356(7)	1.399(7), 1.407(7)
B	27	1.422(5), 1.410(5)	1.366(5), 1.380(5)	1.360(5), 1.348(5)	1.344(7), 1.357(7), 1.349(6)	1.389(6), 1.411(6)	1.364(6), 1.349(6)	1.404(6), 1.402(6)
1	28b	1.422(3)	1.388(3)	1.372(2)	1.368(3)	1.415(3)	1.368(3)	1.416(3)
2	28b	1.466(4), 1.473(4)	1.358(3), 1.353(3)	1.338(4), 1.346(4)	1.376(4), 1.390(4)	1.381(4), 1.371(5)	1.378(4), 1.374(4)	1.394(4), 1.400(4)
3	29	1.465(4)	1.349(4)	1.347(4)	1.375(5)	1.375(5)	1.371(5)	1.389(4)
5	31a	1.422(9)	1.381(9)	1.355(8)	1.38(1)	1.395(20)	1.385(10)	1.43(1)
7	32	1.46(2)	1.35(1)	1.37(1)	1.37(2)	1.37(2)	1.38(2)	1.375(20)
10	31a	1.409(5)	1.386(5), 1.382(5)	1.342(5), 1.340(5)	1.364(7), 1.360(8)	1.360(9), 1.381(9)	1.352(8), 1.352(8)	1.410(6), 1.420(6)
11	38	1.419(3)	1.385(3)	1.376(3)	1.366(3)	1.401(4)	1.364(4)	1.410(3)
15	38	1.417(3)	1.383(2)	1.371(2)	1.368(2)	1.406(3)	1.370(3)	1.409(2)
16	38	1.407	1.414	1.382	1.354	1.418	1.367	1.421
17	38	1.40(1)	1.39(1)	1.38(1)	1.35(1)	1.42(1)	1.35(1)	1.44(1)
18	38	1.418(3)	1.384(3)	1.373(3)	1.363(4)	1.411(4)	1.365(4)	1.412(4)
$[Fe^{II}(bpy^0)(mes)_2]^0$	38	1.481(3)	1.350(3)	1.343(3)	1.381(3)	1.380(4)	1.383(4)	1.397(4)
$[Fe^{II}(bpy^{\bullet-})(mes)_2]^-$	38	1.418(3)	1.385(2)	1.355(2)	1.371(3)	1.400(4)	1.358(4)	1.418(3)

Broken-symmetry DFT calculations can also provide data that allow a distinction to be made between the oxidation state of the central metal ion and the oxidation level of the N,N′-coordinated bpy ligand. We will use this computational tool here for a series of known organometallic compounds of the type $[(Cp)_2M(bpy)]^n$ (M = V, Ti; n = 1−, 0, 1+, 2+) (complexes **1**−**7** and **10**), $[(Cp^*)Co(bpy)]^{0/+}$ (**11** and **12**), $[(\eta^6\text{-toluene})Fe(bpy)]^0$ (**15**), $[(Cp^*)Ru(bpy)]^-$ (**16**), $[(\eta^5\text{-Cp})_2Zr(bpy)]^0$ (**17**), and $[(CO)_3Mn(bpy)]^-$ (**18**). We will also include two 2,2′-biquinoline complexes $[(Cp)_2Ti\text{-}(\text{biquinoline})]^{0,+}$ (**8** and **9**), as shown in Schemes 1 and 2. We will characterize their electronic structures by broken-symmetry DFT calculations and validate these results with the reported experimental data (X-ray crystallographic data, magnetochemistry, EPR spectroscopy, etc.) in an effort to gain *chemical insights* into the nature of these complexes using established computational methodology.

■ RESULTS

1. Experimental Details of Complexes A and B. Because the oxidation state of scandium in most known coordination compounds is III+ with a d^0 electron configuration, we will first consider two organometallic scandium complexes **A** and **B**

containing one (in **A**) or two (in **B**) N,N′-coordinated bpy-type ligands per Sc^{III} ion, namely, diamagnetic $[(\eta^5\text{-Cp}^*)Sc^{III}\text{-}(\text{bpy}^{\bullet-})(\mu\text{-Cl})]_2$ (**A**; S = 0)[26] and $[\{\eta^5\text{-C}_5\text{H}_4(\text{CH}_2)_2\text{N}(\text{CH}_3)_2\}\text{-}Sc^{III}(^m\text{bpy}^{\bullet-})_2]$ (**B**; S = 0, 1).[27] The ground state of **B** has not been determined experimentally, but paramagnetism at ambient temperature has been suggested [S = 1(?)] because of the absence of normal ^{1}H NMR resonances.
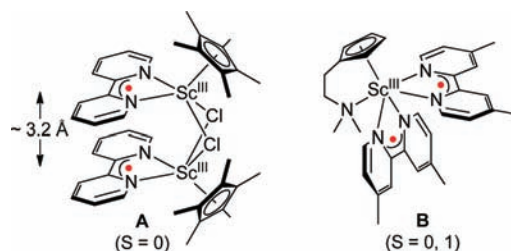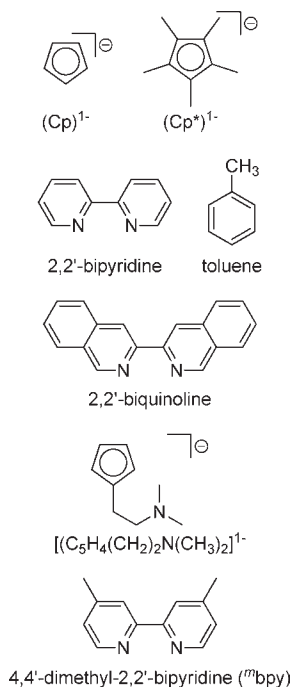

The Evans method with **B** in a benzene solution yielded a magnetic moment of 1.54 μ_B at ambient temperature, possibly indicating a spin equilibrium of a singlet state (S = 0) and a triplet

9775

dx.doi.org/10.1021/ic2005419 |*Inorg. Chem.* 2011, 50, 9773–9793

Scheme 1. Complexes and Spin States under Consideration

$[(\eta^5\text{-Cp*})Sc^{III}(bpy^{\bullet})(\mu\text{-Cl})]_2$	$S = 0$	**A**
$[(\eta^5\text{-C}_5\text{H}_4(\text{CH}_2)_2\text{N}(\text{CH}_3)_2)Sc^{III}(^m bpy^{\bullet})_2]^0$	$S = 0,1$	**B**
$[(\eta^5\text{-Cp})(\eta^3\text{-Cp})V^{III}(bpy^{\bullet})]^0$	$S = {}^1/_2$	**1**
$[(\eta^5\text{-Cp})_2V^{III}(bpy^0)]^{1+}$	$S = 0, 1$	**2**
$[(\eta^5\text{-Cp})_2V^{IV}(bpy^0)]^{2+}$	$S = {}^1/_2$	**3**
$[(\eta^3\text{-Cp})(\eta^5\text{-Cp})Ti^{III}(bpy^{2-})]^{1-}$	$S = {}^1/_2$	**4**
$[(\eta^5\text{-Cp})_2Ti^{III}(bpy^{\bullet})]^0$	$S = 0, 1$	**5**
$[(\eta^5\text{-Cp})_2Ti^{III}(bpy^0)]^{1+}$	$S = {}^1/_2$	**6**
$[(\eta^5\text{-Cp})_2Ti^{IV}(bpy^0)]^{2+}$	$S = 0$	**7**
$[(\eta^5\text{-Cp})_2Ti^{III}(\text{biquinoline}^{\bullet})]^0$	$S = 0, 1$	**8**
$[(\eta^5\text{-Cp})_2Ti^{III}(\text{biquinoline}^0)]^{1+}$	$S = {}^1/_2$	**9**
$[(\eta^5\text{-Cp*})_2Ti^{III}(bpy^{\bullet})]^0$	$S = 0, 1$	**10**
$[(\eta^5\text{-Cp*})Co^{II}(bpy^{\bullet})]^0$	$S = 0$	**11**
$[(\eta^5\text{-Cp*})Co^{II}(bpy^0)]^{1+}$	$S = {}^1/_2$	**12**
$[(\eta^5\text{-Cp*})Co^{III}(bpy^0)Cl]^{1+}$	$S = 0$	**13**
$[(\eta^5\text{-Cp*})Co^{III}(bpy^0)Cl]^0$	$S = {}^1/_2$	**14**
$[(\eta^6\text{-toluene})Fe^{I}(bpy^{\bullet})]^0$	$S = 0$	**15**
$[(\eta^5\text{-Cp*})Ru^{II}(bpy^{2-})]^-$	$S = 0$	**16**
$[(\eta^5\text{-Cp})_2Zr^{IV}(bpy^{2-})]^0$	$S = 0$	**17**
$[(CO)_3Mn(bpy)]^-$	$S = 0$	**18**

Scheme 2. Ligands and Abbreviations

(Cp)$^{1-}$ (Cp*)$^{1-}$

2,2'-bipyridine   toluene

2,2'-biquinoline

$[(C_5H_4(CH_2)_2N(CH_3)_2]^{1-}$

4,4'-dimethyl-2,2'-bipyridine (^{m}bpy)

excited state ($S = 1$). Both **A** and **B** have been characterized by X-ray crystallography,[26,27] and all (bpy) ligands in **A** and **B**

display the characteristic C—C and C—N distances of an N,N'-coordinated π-radical monoanion $(bpy^{\bullet-})^-$ (Table 3), as the original authors have correctly noted. The C1—C1' distances are all in the narrow range of 1.416 ± 0.006 Å. The η^5-coordinated cyclopentadienyl monoanions and the presence of a putative Sc^{III} ion in **A** and **B** render the oxidation level of the bpy ligand as a π-radical monoanion in both complexes. Because these $(bpy^{\bullet-})^-$ anions in solid **A** are π–π interacting at a distance (centroid-to-centroid) of ~3.29 Å (between the two coplanar $(bpy^{\bullet-})^-$ ligands), an intramolecular antiferromagnetic exchange coupling between these two radical anions has been proposed to afford the observed singlet ground state of **A**.[26]

In contrast, the two $(^m bpy^{\bullet-})^-$ radical anions N,N'-coordinated to one Sc^{III} ion in **B** adopt a cis configuration with respect to each other. The two spins can, therefore, couple intramolecularly antiferromagnetically, yielding a singlet ground state, or ferromagnetically, yielding a triplet state. The above experimental results have led the authors[26,27] to the description of the electronic structures of **A** and **B**, as shown above and in Scheme 1. The Sc—N distances in **A** and **B** are long (~2.2 Å) and rule out significant π-bonding effects. We decided to test our DFT methodology by computationally optimizing the geometry of **A** and **B** and calculating their electronic structures (see the Results section). We then apply this approach to more complicated cases as encountered in complexes **1**–**18** (Scheme 1).

*1.2. Complexes **1**–**3***. The vanadium complexes **1**–**3**[28,29] (their structures are shown in Figures 3 and 4) formally constitute an electron-transfer series, where **1** is neutral,[28] **2** is a monocation,[28b] and **3** is a dication;[29] their ground states are reported as $S = {}^1/_2$, 0, and $^1/_2$, respectively. All three compounds have been characterized by single-crystal X-ray crystallography, and the bond distances of the N,N'-coordinated (bpy) ligands are given in Table 3. It is interesting that the cyclopentadienyl anions in **2** and **3** are both bound in an η^5 fashion, whereas in **1**, one of these Cp$^-$ anions is ring-slipped (η^3-coordination) and the other remains η^5-coordinated. The (bpy) structural data clearly indicate that there are neutral bpy^0 ligands in **2** and **3**, rendering the oxidation state of the central vanadium ion as III+ (d^2-electron configuration) in **2** and IV+ (d^1) in **3**. Interestingly, the bpy ligand in neutral **1** exhibits the characteristic geometric features of a π-radical anion (Table 3), which implies the presence of a V^{III} ion (d^2).

The $S = {}^1/_2$ ground state for **1** could be obtained via an intramolecular antiferromagnetic coupling between a high-spin V^{III} (d^2) ion and a $(bpy^{\bullet-})^-$ anion; i.e., the unpaired electron resides in a metal-centered d orbital. Regrettably, its EPR spectrum has not been reported in the original paper.[28] Complex **3** also possesses an $S = {}^1/_2$ ground state. Its X-band solution EPR spectrum in acetonitrile[29] exhibits the typical eight-line spectrum with a large ^{51}V hyperfine coupling constant of 67 × 10^{-4} cm^{-1} characteristic of a V^{IV} ion.

In the original paper, Beckhaus et al.[28b] have not determined the ground state of **2** unambiguously. In principle, it could be a singlet or a triplet state ($S = 0, 1$).

*1.3. Complexes **4**–**10***. Complexes **4**–**7** constitute the four-membered electron-transfer series $[(Cp)_2Ti(bpy)]^{-,0,+,2+}$ of which **5** and **7** have been characterized by single-crystal X-ray crystallography.[30–32] Complex **10** is $[(Cp*)_2Ti(bpy)]^0$ [31a] and complexes **8** and **9** are $[(Cp)_2Ti(\text{biquinoline})]^{0,+}$,[33,34] respectively, which have all been structurally characterized [Cp* represents the monoanion pentamethylcyclopentadienyl(1−)]. Complexes **5**–**10** all contain two η^5-coordinated cyclopentadienyl anions, a central titanium ion, and an N,N'-coordinated bpy- or 2,2'-biquinoline-type ligand.

Inspection of the C1—C1′ bond lengths of the bpy ligands in Table 3 immediately reveals that complexes 5 and 10 contain an N,N′-bound (bpy$^{\bullet-}$)$^-$ π-radical anion. In neutral 8, the 2,2′-biquinoline ligand is also in its N,N′-coordinated, one-electron-reduced form, affording its π-radical anion [biquinolinolate(1−)] with a relatively short C1—C1′ bond at 1.432(2) Å;[33] the same distance in the monocation 9 is long [1.477(5) Å],[34] indicating the presence of a neutral ligand. These structural results imply that the distribution of oxidation states of the central titanium is IV+ (d^0) only in 7; in all other complexes, the titanium ion possesses a III+ (d^1) oxidation state. Concomitantly, the oxidation level of the bpy or biquinoline ligand is neutral in 6, 7, and 9 and monoanionic (π-radical type) in 5, 8, and 10. This distribution is shown in Scheme 1. The monoanionic complex 4 has only been discovered electrochemically, and no structural or spectroscopic data have been reported.[35] We assume here that 4 possesses an $S = \frac{1}{2}$ ground state because of the fact that it contains an uneven number of electrons and is isoelectronic with 1.

The electronic structures of 5, 8, and 10 are very interesting. For complex 5, Stucky et al.[30] have established from magnetic susceptibility (200−350 K) and EPR studies that this species has a triplet excited state that is thermally accessible from the ground-state singlet. The singlet and triplet states are separated by $\sim$600 cm^{-1} ($J = -300$ cm^{-1}, $H = -2J \cdot \vec{S}_1 \cdot \vec{S}_2$, and $S_1 = S_2 = \frac{1}{2}$; its diamagnetic ground state has been confirmed by ^{1}H NMR spectroscopy at ambient temperature in C$_6$D$_6$). The authors of ref 30a concluded from Fenske−Hall molecular orbital calculations that one unpaired electron occupies a molecular orbital that is localized on the Cp$_2$Ti moiety of 5, while the other resides in the lowest-energy π^* orbital of bpy, generating a coordinated π-radical anion (bpy$^{\bullet-}$)$^-$. They also suggested that "the preferred molecular geometries of the singlet and triplet states are not the same". A bent structure is proposed for the singlet configuration (ground state), whereas the C_{2v} structure is favored by a triplet configuration.[30] The calculated dihedral angle α of the two planes TiN$_2$ and the best plane of the N,N′-coordinated (bpy$^{\bullet-}$)$^-$ in 5 is 10.1° (experimental value of 23.2°).[31a] Replacement of the Cp ligands in 5 with Cp* produces complex 10,[31] which exhibits a structure with an α angle of only $\sim$2.5°,[36] implying a very small singlet−triplet energy separation. Solid 10 has been shown to be paramagnetic by EPR spectroscopy, and the intensity of the signal increases with decreasing temperature between 300 and 100 K, possibly implying a triplet ground state for 10. Note that the data sets of the crystal structures of 5 and 10 have been collected at ambient temperature, where the prevalent spin states are $S = 0$ for 5 and $S = 1$ for 10.

Complexes 8 and 9 have been structurally characterized, but their electronic structures have not been determined in detail.[33,34] Complex 8 possesses a singlet or triplet ground state, whereas complex 9 is assumed to possess an $S = \frac{1}{2}$ ground state consistent with that observed for isoelectronic 3.

The structure of paramagnetic 6 ($S_T = \frac{1}{2}$) has not been determined,[30] but that of related 9 has been reported.[34] The electronic structures of both 6 and 9 have been proposed to be typical Ti^{III} species with one unpaired electron in a titanium-centered d orbital and neutral bpy^0 and biquinoline^0 ligands, respectively. An $S = \frac{1}{2}$ ground state is predicted in both cases.

1.4. Complexes 11−14. Kaim et al.[37] have electrochemically investigated the electron-transfer couple [(η^5-Cp*)Co(bpy)]$^{0,+}$ (11 and 12). The neutral complex 11 has been characterized by X-ray crystallography,[38] and it has been reported to possess an $S = 0$ ground state. The structural data of 11 (Table 3) indicate the presence of a (bpy$^{\bullet-}$)$^-$ π-radical anion, which implies a central Co^{II}

ion ($S_{Co} = \frac{1}{2}$) that is intramolecularly antiferromagnetically coupled to the radical, affording the observed singlet ground state. This description signifies a singlet diradical electronic structure for 11 ([(η^5-Cp*)Co^{II}(bpy$^{\bullet-}$)]^0, $S = 0$).

Compound 12, namely, [(η^5-Cp*)Co(bpy)]$^+$ ($S_T = \frac{1}{2}$), has only been characterized in solution by EPR spectroscopy.[37] It displays a rhombic signal ($g_1 = 2.277$, $g_2 = 2.094$, and $g_3 = 1.972$) with large ^{59}Co hyperfine splitting parameters ($A_1 = 60$ G, $A_2 = 28$ G, and $A_3 = 30$ G) typical for a low-spin Co^{II} ion (d^7, $S_{Co} = S_T = \frac{1}{2}$). This indicates that, although the structure is not known, a neutral bpy^0 ligand should be present.

The synthetic precursor to 12 is the diamagnetic species [(η^5-Cp*)Co^{III}(bpy^0)Cl]$^+$ (13)[39] (its structure is not known), which contains a neutral bpy^0 ligand and a low-spin central Co^{III} ion (d^6, $S_{Co} = 0$). The one-electron-reduced form [(η^5-Cp*)Co^{II}(bpy^0)Cl]^0 (14) has only been generated electrochemically in solution,[37] and its electronic structure has not been established, but it is rather unstable and loses a chloride ion, generating the monocation 12.

1.5. Complex 15. Diamagnetic [(η^6-toluene)Fe(bpy)]^0 (15)[14] is isoelectronic with complex 11. The structure of 15 has been reported,[14] and the metrical details of the bpy ligand (Table 3) clearly display the characteristics of a π-radical anion (as in 11). This formulation predicts the singlet diradical electronic structure [(η^6-toluene)Fe^I(bpy$^{\bullet-}$)]^0 ($S = 0$). The original authors[14] have preferred a description where "extensive π-backbonding to a [(bpy^0)] ligand from a first-row transition metal" prevails and accordingly assigned a formal metal oxidation state of zero to iron, suggesting a closed-shell singlet description for 15.

1.6. Complex 16. The monoanion in complex 16, namely, [(η^5-Cp*)Ru(bpy)]$^-$, is also diamagnetic and isoelectronic with 15.[40] This species has been generated by the reduction of [(Cp*)(bpy^0)Ru^{II}Cl] with an excess of KC$_8$ in THF. Its crystal structure has been determined,[40] and on the basis of the observation of a normal ^{1}H NMR spectrum, a singlet ground state has been established, but the electronic structure of this species has not been determined in great detail. There are two crystallographically independent anions in the unit cell. The N,N′-coordinated bpy displays the characteristics of a highly reduced neutral bpy^0 ligand (Table 3), namely, a radical monoanion (bpy$^{\bullet-}$)$^-$ or, even more appropriately, a dianion (bpy^{2-})$^{2-}$. Thus, the electronic structure of 16 may be described as either [(η^5-Cp*)Ru^I(bpy$^{\bullet-}$)]$^-$ or [(η^5-Cp*)Ru^{II}(bpy^{2-})]$^-$, i.e., a singlet diradical or a closed-shell singlet. This is a typical situation where only careful DFT calculations will allow us to discriminate between the two formulations.

1.7. Complex 17. The synthesis of the zirconium complex 17 (Figure 15) has been reported.[30,41a,41b] From its normal ^{1}H NMR spectrum, it has been suggested that 17 is diamagnetic ($S = 0$ ground state). It is, therefore, unknown which of the following possibilities describes the electronic structure of 17 correctly: [(η^5-Cp)$_2$Zr^{II}(bpy^0)]^0, [(η^5-Cp)$_2$Zr^{III}(bpy$^{\bullet-}$)]^0, or [(η^5-Cp)$_2$Zr^{IV}(bpy^{2-})]^0.

The crystal structure of 17 has also been reported.[41c] It displays a highly distorted N,N′-coordinated bpy ligand with dearomatization of the rings and a short C1—C1′ bond at 1.40(1) Å. The authors of ref 41c interpret these distortions as resulting from "donation of electron density from zirconium to antibonding levels of the (bpy) unit". They imply the presence of a d^2 electron configuration of zirconium: [(Cp)$_2$Zr^{II}(bpy^0)]. The structure of [(Cp)$_2$Zr(bpy)(OTf)](OTf) ($S = 0$) has also been reported;[41d] it clearly contains a neutral bpy^0 ligand [C1—C1′ at

1.48(2) Å] and, therefore, is best described by the electronic structure $[(Cp)_2Zr^{IV}(bpy^0)(OTf)]^+$.

*1.8. Complex **18**.* The synthesis, crystal structure, and DFT calculations for $[(Na(bpy^0)][Mn(CO)_3(bpy)]\cdot Et_2O$ ($S = 0$) have recently been reported.[42a] The most interesting feature of the crystal structure is the presence of a neutral bpy^0 ligand coordinated to the sodium cation and a reduced $(bpy^{\bullet-})^-$ π-radical anion coordinated to the manganese atom (Table 3). The electronic structure of the anion **18** could then be described as $[Mn^0(CO)_3(bpy^{\bullet-})]^-$, where the singlet diradical is composed of a central Mn^0 (d^7, $S_{Mn} = {}^1/_2$) and an antiferromagnetically coupled π-radical anion $(bpy^{\bullet-})^-$. The reported closed-shell DFT calculations[42a] revealed a highest occupied molecular orbital (HOMO) with 57% bpy character and 29% manganese character; these restricted Kohn–Sham (RKS) calculations are not suited for identifying a singlet diradical configuration as is invoked by the above electronic structure description. Therefore, we have repeated the calculations using the broken-symmetry formalism in an attempt to identify a singlet diradical solution for **18** (see below). Interestingly, the structure of the related compound $[Mn^I(CO)_3(bpy^0)I]^0$ ($S = 0$) reveals the presence of a *neutral* bpy^0 ligand, rendering the oxidation state of the central Mn ion as I+ (d^6, $S_{Mn} = 0$).[42b] Anion **18** may also be described by the following resonance structures: $[(CO)_3Mn^{I-}(bpy^0)]^-$ (Mn^{I-}, d^8, $S_{Mn} = 0$) $\leftrightarrow [(CO)_3Mn^0(bpy^{\bullet-})]^-$ (Mn^0, d^7, $S_{Mn} = {}^1/_2$) $\leftrightarrow [(CO)_3Mn^{I+}(bpy^{2-})]^-$ (Mn^{I+}, d^6, $S_{Mn} = 0$). The authors in ref 42a describe their results on **18** as follows: "[t]he data are consistent with a substantial localization of electron density in the π^* LUMO of the Mn-bound bpy ligand and the formulation of $[Mn(CO)_3(bpy)]^{1-}$ as a compound with fully delocalized π-bonding in the Mn(bpy) metallocycle and strong (bpy)Mn $\rightarrow$ CO π-backdonation". This description is equivalent to the latter two above resonance structures and formally involves electron π donation from a $(bpy^{2-})^{2-}$ to a Mn^+ ion with concomitant $(bpy^{2-})Mn^{I+} \rightarrow$ CO π backdonation; the first of the three above resonance structures involving a bpy^0 ligand and a Mn^{I-} ion plays a very minor role.

2. DFT Calculations. The geometries of all complexes were optimized using the B3LYP hybrid functional for spin-unrestricted $M_S \approx S = x$ systems, where the crystallographically determined molecular structures (if available) were used as the starting geometry. In general, the agreement between the experimental and calculated intraligand bond distances is excellent. The calculated bond lengths and other structural details are available in the Supporting Information in the form of molecular *xyz* coordinates. The M–X bond lengths are 0.06–0.09 Å longer than the experimental values, a feature that is typical of the B3LYP functional. The calculated C1–C1′ bond distances of the bpy ligands in complexes **A**, **B**, and **1**–**18** are given in Table 4.

*2.1. Complexes **A** and **B**.* The geometry-optimized structures for the $S = 0$ and 1 spin states of complex **A** are shown in Figure 2. Only the closed-shell ($S = 0$) optimized structure was found to be in excellent agreement with the experimental structure.[26] The metrical data of both bpy ligands display the typical π-radical monoanionic $(bpy^{\bullet-})^-$ character. An intramolecular π–π interaction between the two N,N′-coordinated $(bpy^{\bullet-})^-$ ligands is observed, with a distance of 3.28 Å between the centroids of the two bpy ligands (experimental value is 3.30 Å[26]). The HOMO of **A**, shown in Figure 2a, is shared across both $(bpy^{\bullet-})^-$ ligands. This HOMO has 82.4% bpy character and only 15.0% scandium character. The spins of the two electrons in this HOMO, formally from the two $(bpy^{\bullet-})^-$ radical pairs, are in an antiparallel alignment (Pauli principle). Thus, **A** possesses a diamagnetic ground state. The five empty metal d orbitals are at higher energy,

Table 4. Calculated and Experimental C1–C1′ Bond Distances (Å) and Corresponding Assignment of the Oxidation Level of N,N′-Coordinated bpy Ligands

complex	exptl	calcd	assignment
A	1.419(9), 1.415(9)	1.439	$(bpy^{\bullet-})^-$
B	1.422(5), 1.410(5)	1.432, 1.432	$(bpy^{\bullet-})^-$
1	1.423(3)	1.424	$(bpy^{\bullet-})^-$
2	1.466(4), 1.473(4)[a]	1.476	bpy^0, bpy^0
3	1.465(4)	1.472	bpy^0
4	nd[b]	1.395	$(bpy^{2-})^{2-}$
5	1.422(9)	1.427	$(bpy^{\bullet-})^-$
6	nd[b]	1.479	bpy^0
7	1.46(2)	1.476	bpy^0
8	1.432(2)	1.438	$(biquinoline^{\bullet-})^-$
9	1.484(5),[c] 1.477(5)[d]	1.484	$biquinoline^0$
10	1.409(5)	1.424	$(bpy^{\bullet-})^-$
11	1.419(3)	1.428	$(bpy^{\bullet-})^-$
12	nd[b]	1.474	bpy^0
13	nd[b]	1.473	bpy^0
14	nd[b]	1.484	bpy^0
15	1.417(3)	1.427	$(bpy^{\bullet-})^-$
16	1.413(9), 1.401(9)	1.408	$(bpy^{2-})^{2-}$
17	1.40(1)	1.425	$(bpy^{2-})^{2-}$
18	1.418	1.419	$(bpy^{\bullet-})^-$

[a] There are two crystallographically independent monocations in the crystals of **2**. [b] nd = not determined. [c] From PF_6^- salt. [d] From I_3^- salt.

as was expected for a d^0 electron configuration at each Sc^{III} ion. Therefore, the present DFT calculations validate the structure and proposed ground state ($S = 0$) of **A**.

We have also optimized the structure of **A** for a triplet excited state. This structure is shown in Figure 2b. Interestingly, the bond lengths of the bpy ligands still indicate π-radical monoanionic character $(bpy^{\bullet-})^-$, but in contrast to the structure of the singlet state of **A**, the π–π interaction between the two $(bpy^{\bullet-})^-$ radicals does not exist anymore in its triplet excited state (centroid-to-centroid distance of 3.65 Å). The two planar $Sc(bpy^{\bullet-})$ moieties are now twisted away from each other so that the lowest-energy π^* orbitals of the $(bpy^{\bullet-})^-$ ligands cannot overlap and the two spins of the $[Sc(bpy^{\bullet-})]_2$ unit order in a ferromagnetic fashion [the plane(bpy1)–centroid(bpy1)–centroid(bpy2) angle is 68.1°]. The energy difference between the geometry-optimized singlet ground state and the triplet excited state is calculated to be 6.4 kcal/mol. The two unpaired electrons in the triplet state reside in the bonding and antibonding combinations of the π^* orbitals of the two $(bpy^{\bullet-})^-$ ligands.

The molecular structure of **B** has been optimized using a RKS closed-shell ($S = 0$) and a broken-symmetry BS(1,1) ($M_S = 0$) approach; the latter solution was found to be more stable by 3.6 kcal/mol and is shown in Figure 3. The optimized geometry of the broken-symmetry solution for **B** is in excellent agreement with the experimental geometry[27] and indicates the presence of two $(bpy^{\bullet-})^-$ radical anions and a central Sc^{III} ion with a d^0 electron configuration, as revealed by the Mulliken spin-density distribution (α spin of 0.89 and β spin of -0.90, each on the bpy ligands). The two SOMOs possess 89.4% and 89.9% ligand character for the first and second $(bpy^{\bullet-})^-$ ligands, respectively. The geometry of the triplet excited state of **B** is nearly identical with that of the ground state ($M_S = 0$; Figure 3). The singlet–triplet energy gap has been
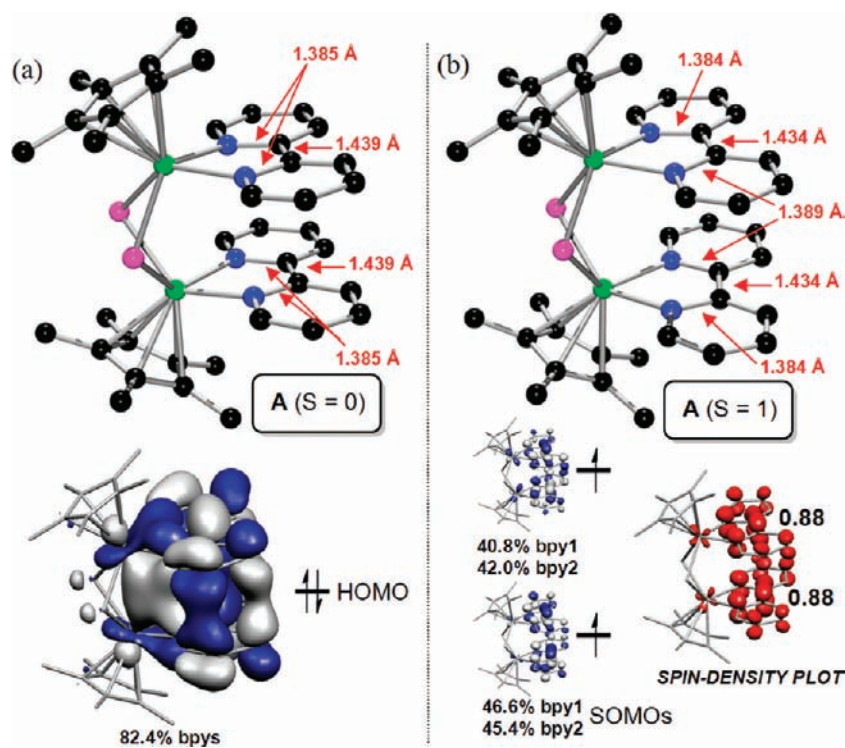
9778

dx.doi.org/10.1021/ic2005419 |*Inorg. Chem.* 2011, 50, 9773–9793

Figure 2. Calculated structures of **A**: (a) $S = 0$, including the HOMO (isoelectron density surface 98.0%) of **A**; (b) $S = 1$, including the two SOMOs of **A** and the spin-density distribution plot (Mulliken). Color code: green, scandium; pink, chlorine; blue, nitrogen; black, carbon.
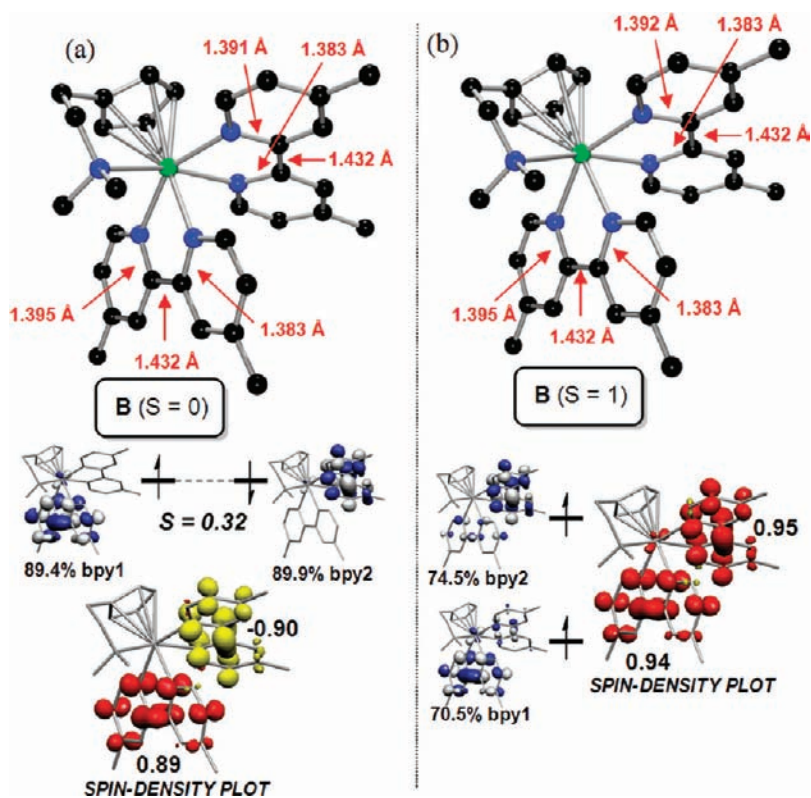

Figure 3. Calculated structures of **B** [(a) $S = 0$ and (b) $S = 1$] and the SOMOs and spin-density distribution (Mulliken). The overlap integral (S) in part a is the calculated spatial overlap between the α- and β-spin components of the magnetic orbitals. Color code: green, scandium; blue, nitrogen; black, carbon.
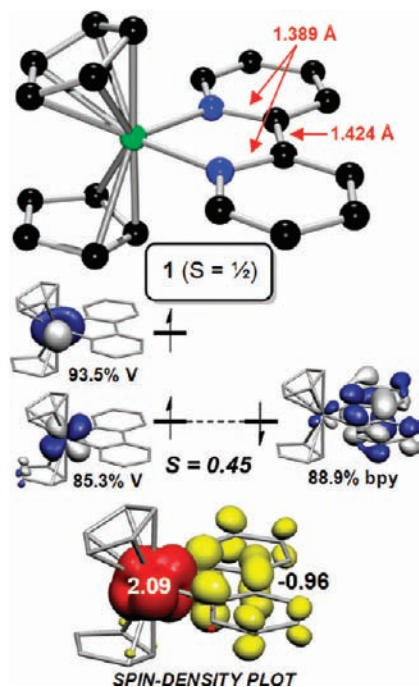
Figure 4. Calculated structure of **1** ($S = {}^1/_2$), the SOMOs (S represents the overlap integral), and the spin-density distribution (Mulliken). Color code: green, vanadium; blue, nitrogen; black, carbon.

Table 5. Ring-Slippage Parameters of the η^3-Cp$^-$ Rings of 1 and 4 (See Reference 28b for Definition of the Ring-Slippage Parameters)

compound	Δ (Å)	Ψ (deg)	ΔM$-$C$_{ave}$ (Å)	Ω (deg)
1 (experimental)[28b]	0.88	22	0.56	8.3
1 (calculated)	0.81	20	0.52	8.0
4 (calculated)	0.23	6	0.15	1.4

An antiferromagnetic coupling constant (J) of -895 cm^{-1} has been calculated.[43] Consistent with the magnitude of the calculated antiferromagnetic coupling constant, the overlap integral (S) between the two magnetic orbitals is 0.45, which indicates a strong interaction.

The three limiting electronic structure possibilities of **1**, given its experimentally established $S = {}^1/_2$ ground state, are (a) low-spin V^{II} (d^3) with a neutral bpy^0 ligand, (b) high-spin V^{III} (d^2, $S_V = 1$) antiferromagnetically coupled to a (bpy$^{\bullet-}$)$^-$ radical anion providing an overall spin $S = {}^1/_2$, and (c) low-spin V^{III} (d^2, $S_V = 0$) with a bpy-centered radical anion. Electronic structure description (a) is ruled out based on the observed bpy metrical parameters, which indicate the presence of a (bpy$^{\bullet-}$)$^-$ radical anion. Electronic structure description (c) is ruled out because, in this formulation, there is no driving force for the observed ring slippage of one of the Cp$^-$ ligands. On the basis of the X-ray crystal structure alone, electronic structure description (b) is favored because a high-spin V^{III} (d^2, $S_V = 1$) requires occupation of a d orbital that is π antibonding with two carbon atoms of one Cp ring,[45] providing the driving force for the ring slippage; occupation of this d orbital also provides a mechanism for a productive antiferromagnetic coupling interaction with the singly occupied π^* orbital of the (bpy$^{\bullet-}$)$^-$ ligand, allowing the central vanadium to be in-plane with the average plane of the bpy carbon and nitrogen atoms (cf. complex **4**, vide infra). It is reassuring that the broken-symmetry BS(2,1) calculations reproduce this predicted electronic structure description, and the ring-slippage parameters of the optimized geometry agree very well with the experimental values (Table 5).

In summary, the molecular and electronic structure of the 17-electron species **1** is best described as $[(\eta^3\text{-Cp})(\eta^5\text{-Cp})\text{V}^{III}(\text{bpy}^{\bullet-})]^0$ with an $S_T = {}^1/_2$ electronic ground state, which is attained via a strong intramolecular antiferromagnetic coupling between a high-spin V^{III} ion (d^2, $S_V = 1$) and a (bpy$^{\bullet-}$)$^-$ π-radical anion ($S_L = {}^1/_2$). Our data do not corroborate the proposed electronic structure of **1**, namely, $[\text{Cp}_2\text{V}^{II}(\text{bpy}^0)]^{0,28b}$ and instead are consistent with the electronic structure description described above.

2.3. Complex **2**. The geometry of the monocation $[\text{Cp}_2\text{V}(\text{bpy})]^+$ (**2**) was optimized by an unrestricted Kohn$-$Sham (UKS) calculation ($S = 0$) starting from the experimental atom coordinates. Excellent agreement between the experimental and calculated structures (Figure 5) has been achieved. There are two η^5-bound Cp$^-$ anions and a neutral N,N′-coordinated bpy present. The central vanadium ion possesses a III+ oxidation state and its electronic configuration is low-spin (d$_{xy}{}^2$; the HOMO is 83.7% vanadium in character). The calculated C1$-$C1′ distance of the bpy ligand in the cation **2**, at 1.476 Å (Table 3), agrees well with experiment and unambiguously indicates the presence of a neutral bpy^0 ligand. Attempts to find a broken-symmetry $[\text{BS}(1,1), M_S = 0]$ solution failed, in each case converging to the same solution described above.

We have also calculated and optimized the structure of the paramagnetic ($S = 1$) excited state of the monocation in **2** (Figure 5). Despite using a starting geometry with two η^5-bound Cp$^-$ ligands,

calculated to be $\sim$590 cm^{-1} ($J = -293$ cm^{-1}).[43] This is in very good agreement with experiment, where it was shown by ^{1}H NMR spectroscopy (Evans method) that **B** is paramagnetic (1.54 μ_B per Sc ion) in a benzene solution at ambient temperature. Antiferromagnetic spin exchange coupling between two cis-configured bidentate ligand radicals (e.g., semiquinonates) in an octahedral complex mediated by a diamagnetic metal ion has been described in the past.[44]

In summary, the agreement between the above DFT calculations and the experimental data on complexes **A** and **B** convincingly demonstrate the power of this methodology.

2.2. Complex **1**. Geometry optimization of **1** [B3LYP, BS-(2,1); $S = {}^1/_2$] using the experimental atom coordinates as the starting point faithfully reproduces the experimental structure, including the η^3-binding mode (ring slippage) of one Cp$^-$ ligand and the more symmetric η^5 mode of the other Cp$^-$ ligand. Interestingly, a geometry optimization using the atom coordinates of **2** (containing two η^5-bound Cp$^-$ ions) as the starting geometry also affords a structure with one η^5-bound Cp$^-$ anion and one η^3-bound Cp$^-$ anion, but the relative positions between the η^3-Cp and bpy ligands differ from those of the first optimized structure. The latter solution represents a local energy minimum; it is $\sim$5 kcal/mol higher in energy than the first. Clearly, the ring slippage in **1** has an electronic origin.

The N,N′-coordinated bpy ligand in **1** displays the characteristic features of a π-radical anion (bpy$^{\bullet-}$)$^-$ (Tables 3 and 4). The central vanadium ion must, therefore, possess a III+ oxidation state (d^2, $S_V = 1$). The calculated Mulliken spin-density distribution in **1** (Figure 4) is in excellent agreement with this formulation, where a single electron is localized on the bpy ligand and two unpaired electrons are located at the central V^{III} ion. The intramolecular coupling between these three electrons is antiferromagnetic, yielding the observed $S = {}^1/_2$ ground state, with the unpaired electron residing in a metal-centered $\sim$d$_{xy}$ orbital.
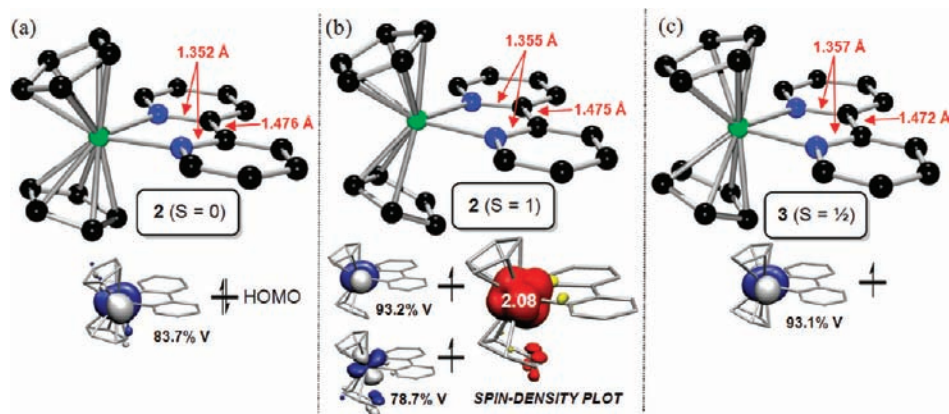
Figure 5. Calculated structures of **2** [(a) S = 0; (b) S = 1] and **3** [(c) S = $^{1}/_{2}$]: (a) HOMO of **2** (S = 0; (b) SOMOs and spin-density distribution of **2** (S = 1); (c) SOMO of **3** (S = $^{1}/_{2}$). Color code: green, vanadium; blue, nitrogen; black, carbon.

the final optimized structure contains one η^3-bound Cp^- ligand and one η^5-bound Cp^- ligand; the bpy bond lengths remain consistent with the formulation bpy^0. Thus, ring slippage is observed in the excited state, as expected for a high-spin d^2 configuration (cf. **1**). The triplet structure of **2** is 2 kcal/mol higher in energy than the diamagnetic ground-state structure that contains two η^5-bound Cp^- anions (Figure 5). Note that the singlet and triplet geometries of **2** have been calculated for a single molecule in the gas phase. In the solid state, ring slippage may not be observed because of steric hindrance and, consequently, the S = 1 excited state may not be accessible up to room temperature. Single-point calculations of the crystal-structure geometries of **2**[46] (with two η^5-bound Cp^- ligands) reveal a singlet−triplet energy separation of 14−16 kcal/mol, reflecting the large driving force for ring slippage in the case of a high-spin d^2 configuration. In both the ground- and excited-state structures, the bpy ligand is neutral.

*2.4. Complex **3***. The geometry of the dication $[Cp_2V(bpy)]^{2+}$ (**3**) was optimized by a UKS calculation (S = $^{1}/_{2}$) starting from the experimental geometry (Figure 5c).[29] Excellent agreement between experiment and theory is observed. There are two η^5-bound Cp^- anions and a neutral bpy^0 ligand present (Table 3), which allows assignment of a formal oxidation state of IV+ to the central vanadium ion (d^1). The calculated electronic structure of the dication confirms this notion: the ligands Cp^- and bpy carry essentially no spin density, whereas the central vanadium ion has one unpaired electron in the d_{xy} orbital (93% vanadium character). This nicely corroborates the experimental EPR spectrum of **3**.[29]

*2.5. Complex **4***. Figure 6 shows the calculated structure of the monoanion $[(\eta^5\text{-}Cp)(\eta^3\text{-}Cp)Ti^{III}(bpy^{2-})]^-$ (**4**; S = $^{1}/_{2}$). One η^5-coordinated Cp^- and one η^3-coordinated Cp^- are identified, although the extent of ring slippage is lower than that in **1** (Table 5). The SOMO possesses 90.5% titanium d character, indicating that the central metal is a Ti^{III} (d^1) ion. This oxidation state implies the presence of an N,N′-coordinated $(bpy^{2-})^{2-}$ dianion, as is verified by the fact that the doubly occupied HOMO of **4** possesses 80% bpy character and only 13% metal d character. The titanium d character in the HOMO of **4** indicates that a $(bpy^{2-})^{2-}$ dianion is a π donor and, consequently, the calculated C1−C1′ distance (1.395 Å) is slightly longer than that in the sodium- and potassium-coordinated $(bpy^{2-})^{2-}$ complexes. The Mulliken spin-density distribution (Figure 6) shows that ∼1.26 unpaired electrons are present at the Ti^{III} center and only −0.26 on the $(bpy^{2-})^{2-}$ ligand.

Complexes **4** and **1** are formally isoelectronic; however, in **4**, we are assigning a ligand oxidation level of $(bpy^{2-})^{2-}$, and in **1**, we
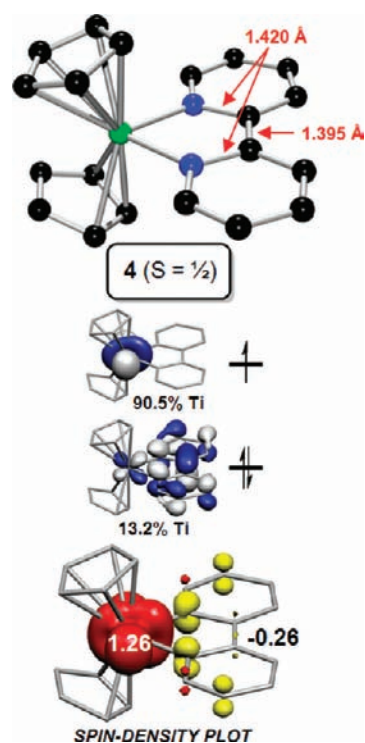

Figure 6. Calculated structures of **4** (S = $^{1}/_{2}$) and the SOMO, HOMO, and spin-density distribution (Mulliken). Color code: green, titanium; blue, nitrogen; black, carbon).

are assigning the level $(bpy^{\bullet-})^-$. This difference is consistent with the higher-energy d orbitals of titanium compared to vanadium. The extent to which ring slippage of one Cp^- ligand occurs is dependent upon the occupation of the energetically second-lowest d orbital: in the case of **1**, this orbital is occupied by a single unpaired electron, and in the case of **4**, this orbital is less than half-occupied, in this case via π donation from the $(bpy^{2-})^{2-}$ dianion. This interpretation is consistent with the extent of ring slippage of one Cp^- ligand being much greater in **1** than in **4** (Table 5).

*2.6. Complex **5***. The geometry of diamagnetic **5** was optimized by a closed-shell (S = 0, RKS) and, alternatively, a broken-symmetry BS(1,1) calculation. It was found that the BS(1,1) solution is 7.9 kcal/mol lower in energy than the closed-shell solution. The optimized structure agrees well with the experimental one (Figure 7).
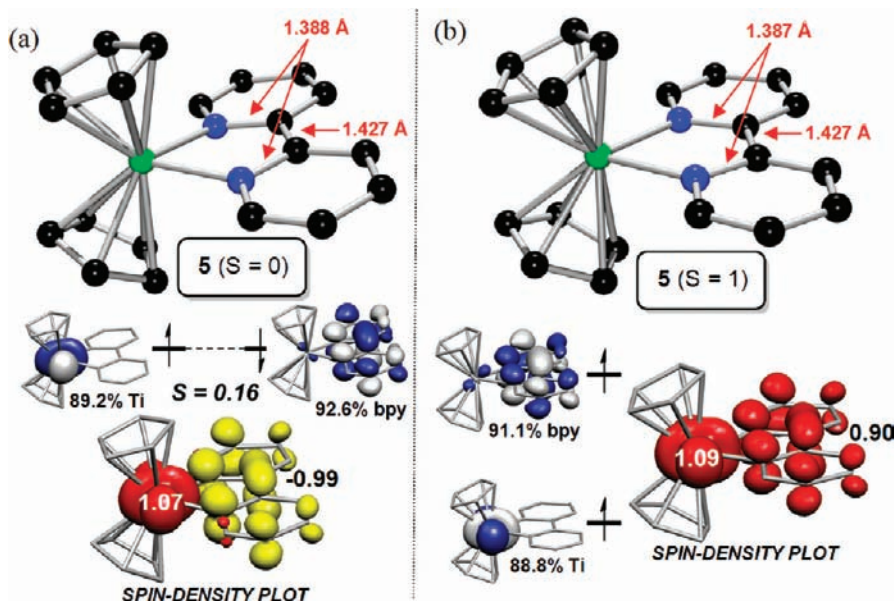
Figure 7. Calculated structure of **5** [(a) $S = 0$; (b) $S = 1$] and the SOMOs and spin-density distribution plots (Mulliken). Color code: green, titanium; blue, nitrogen; black, carbon).

Thus, the neutral molecules in **5** are singlet diradicals with one unpaired electron in the π^* orbital of bpy and the other unpaired electron in a metal-centered d orbital (d_{xy}^1, 88.5% titanium). It is gratifying that the calculated geometry of the Ti(bpy$^{\bullet -}$) unit is bent with a dihedral angle α of 10.3° (exptl = 23.3°) between the TiN$_2$ plane and the best plane of the bpy. The presence of the (bpy$^{\bullet -}$)$^-$ π-radical anion is identified by the calculated short C1—C1' distance of 1.427 Å [exptl = 1.422(9) Å].

The optimal structure of the triplet excited state ($S = 1$, UKS) of **5** has also been calculated. As shown in Figure 7, the presence of (bpy$^{\bullet -}$)$^-$ is identified by the short C1—C1' bond length (1.427 Å). The Ti(bpy$^{\bullet -}$)$^-$ unit is now flat (the dihedral angle between the TiN$_2$ and bpy planes is at ∼0°), as has been proposed based on Fenske—Hall molecular orbital calculations[30] and which is consistent with the experimental structures of isoelectronic **8**[33] and **10**,[31] which are proposed to be ground-state triplets. The calculated Mulliken spin-density distribution shown in Figure 7 displays the π^*-ligand SOMO and the half-filled metal-centered d orbital; they are orthogonal with respect to each other and constitute a ferromagnetic superexchange coupling, yielding the observed $S = 1$ excited state.

Using the Yamaguchi approach,[43] we have calculated the energy separation between the diamagnetic ground state and the energetically low-lying triplet excited state of **5** to be ∼300 cm^{-1} ($J \approx -150$ cm^{-1}). This is in reasonable agreement with experiment ($J \approx -300$ cm^{-1}).[30]

Gratifyingly, our DFT methodology has reproduced the molecular and electronic structure of **5** obtained by experiment. The previous (mainly experimentally based) assignment of **5** as [(η^5-Cp)$_2$Ti^{III}(bpy$^{\bullet -}$)]^0 is corroborated by the present DFT calculations. Our calculations even reproduce the bent nature of the Ti(bpy$^{\bullet -}$) unit and its flat structure for the triplet excited state (see also complexes **8**, **10**, and **17** vide infra). The origin of the bending of the bpy plane away from the TiN$_2$ plane is understood by the fact that this bending lowers the symmetry from C_{2v} to C_s, allowing the bpy π^* orbital (A' symmetry) to overlap with the singly occupied d_{xy} orbital (A' symmetry), forming a weak σ-bonding interaction between the two orbitals

that is maximized at $\alpha = 90°$. Given that the σ-bonding interaction between the nitrogen-centered (formally sp^2) lone pairs and the central titanium ion is maximized at $\alpha = 0°$, it appears that balancing these opposing interactions is responsible for the observed α angle. It is noteworthy that, in C_{2v} symmetry, the d orbital has A$_1$ symmetry, whereas the bpy π^* orbital has B$_1$ symmetry, precluding their interaction in this point group. This bending contrasts the planarity of **1** because the high-spin d^2 electronic configuration of the central vanadium in **1** results in the occupation of a d orbital that has the correct symmetry and spatial distribution for a productive overlap with the bpy π^* orbital without deviating from $\alpha = 0°$; this interaction is stronger than the bonding interaction in **5**, as is expected from the spatial distribution of the orbitals involved and confirmed by the calculated J values[43] for these compounds ($J = -895$ cm^{-1} in **1** and -146 cm^{-1} in **5**).

*2.7. Complexes **6** and **7***. The structures of the paramagnetic monocation **6** ($S = {}^1/_2$) and of the diamagnetic dication **7** ($S = 0$) have been optimized by UKS calculations using the atom coordinates of **7** as the starting geometry (Figure 8). The structural features of the N,N'-coordinated bpy ligands clearly display the characteristics of the neutral oxidation level bpy^0 in both cases. Also, both Cp$^-$ monoanions are coordinated in an η^5 fashion in both **6** and **7**. Therefore, the central metal ion must have a III+ oxidation state (d^1) in **6** and a IV+ oxidation state (d^0) in **7**. This is nicely borne out by the Mulliken spin-density distribution (Figure 8), which shows a single unpaired electron in a metal d orbital for **6** but no spin density on any atom in the dication **7**. Note that the calculated structure of **7** agrees well with the experimental one;[32] the structure of **6** has not been reported. The LUMO of **7** becomes the SOMO in **6**; both are metal-centered d orbitals with 89.0% titanium character in **6** and 86.2% in **7**. These results corroborate the proposals by the previous authors in refs 30 and 32.

*2.8. Complex **8***. The geometry of complex **8** ($S = 0$) has been calculated using a closed-shell RKS and a BS(1,1) approach. The broken-symmetry solution was found to be 15 kcal/mol lower in energy than the closed-shell solution (Figure 9); the latter will
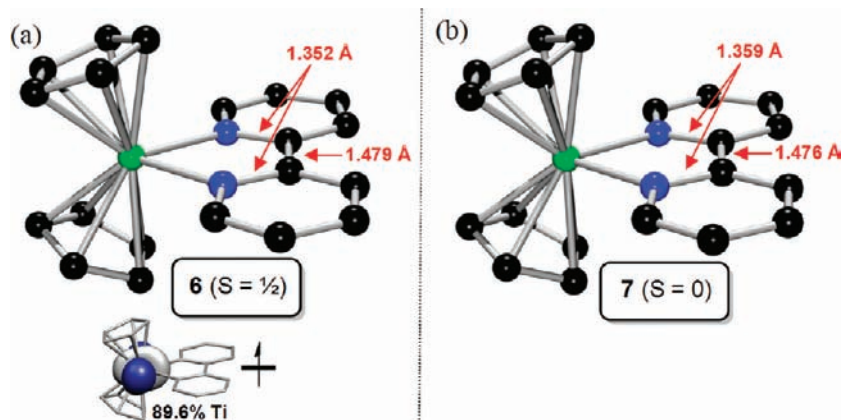
Figure 8. Calculated structures of (a) **6** ($S = {}^1/_2$) and (b) **7** ($S = 0$) and the SOMO of **6**. Color code: green, titanium; blue, nitrogen; black, carbon.
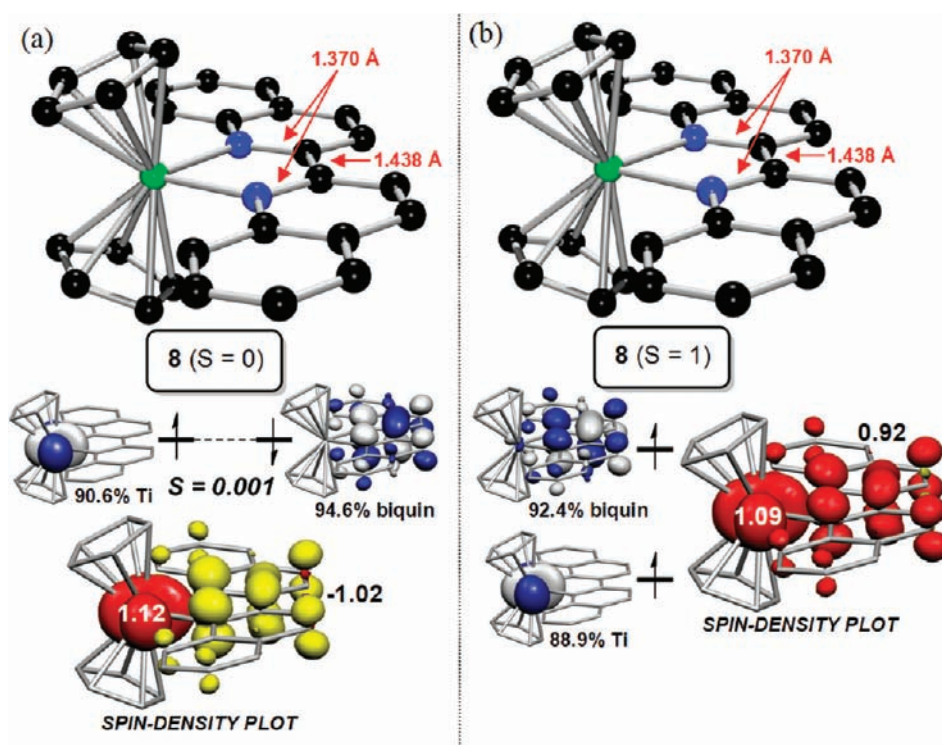

Figure 9. Calculated structure of **8** [(a) $S = 0$; (b) $S = 1$], including spin-density distribution plots (Mulliken) and frontier molecular orbitals. Color code: green, titanium; blue, nitrogen; black, carbon.

not be considered further. We have also optimized the geometry of the triplet state of **8** by a UKS calculation with atom coordinates of **8**[33] as the starting point. The bond distances and angles of the singlet and triplet structures are nearly identical. In both cases, the presence of a 2,2′-biquinolinate π-radical anion is established by a short C1—C1′ distance at 1.438 Å [Table 3; experimental value 1.432(2) Å]; the Cp⁻ anions are all bound in an η^5 fashion. The singlet and triplet states are nearly degenerate, with the singlet state being lower in energy by only ∼0.02 kcal/mol. The small singlet−triplet gap corresponds to a small calculated antiferromagnetic coupling constant J of only −7 cm⁻¹, which is significantly smaller than is observed (−300 cm⁻¹) and calculated (−150 cm⁻¹) for analogous **5**. Notably, the Ti-(biquinolinate•⁻) moiety is flat in both the singlet and triplet

states, whereas in **5**, the former is bent and only the latter triplet state possesses a flat Ti(bpy•⁻) unit.

The Mulliken spin-density distributions of the singlet and triplet states of **8** (Figure 9) show that, in each case, one unpaired electron resides in the biquinoline π* orbital and the other resides in a metal-centered d orbital. We propose that more magnetochemical and spectroscopic data for **8** are needed in order to test the validity of the above calculations.

*2.9. Complex **9***. The geometry-optimized (UKS) structure of the cation [(Cp)₂Ti(biquinoline)]⁺ (**9**), where the experimental atom coordinates[34] were used as the starting geometry, clearly shows the presence of a neutral 2,2′-biquinoline ligand and two Cp⁻ anions, which renders the central metal ion Ti^{III} d¹ (the calculated structural parameters are in excellent agreement with

9783

dx.doi.org/10.1021/ic2005419 |*Inorg. Chem.* 2011, 50, 9773–9793

the experimental ones; see Figure 10). The electronic structure description $[(Cp)_2Ti^{III}(biquinoline)]^+$ ($S_T = {}^1/_2$) is confirmed by a Mulliken spin-density distribution analysis, which places a single unpaired electron in a metal d orbital. This result gives us confidence that the electronic structure of $[(Cp)_2Ti^{III}(bpy^0)]^+$ (**6**, $S_T = {}^1/_2$) is similar.

2.10. Complex **10**. Calculations on the singlet state of $[(Cp^*)_2Ti^{III}(bpy^{\bullet-})]^0$ (**10**; see Figure 11) have been performed in a fashion completely analogous to those described for **5** and **8** (see Figures 7 and 9). The broken-symmetry solution BS(1,1) was found to be 12.7 kcal/mol lower in energy than the closed-shell singlet RKS solution. The optimized geometry displays the geometrical features of an N,N′-coordinated bpy π-radical anion. Both Cp^{*-} ligands are bound in an η^5 fashion, and the $Ti(bpy^{\bullet-})$ moiety is flat. These results agree nicely with experiment. The geometry of the triplet state of **10** has also been optimized ($S = 1$,
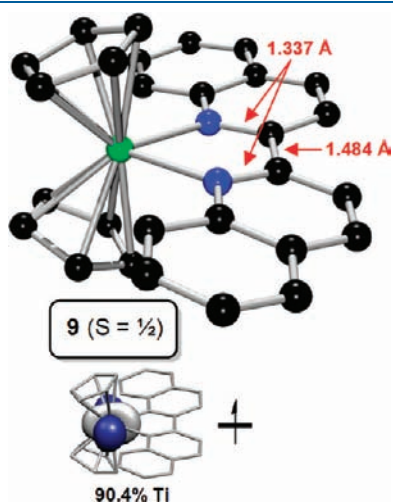

Figure 10. Calculated structure of the cation **9** and its SOMO. Color code: green, titanium; blue, nitrogen; black, carbon.

UKS). The singlet and triplet structures are virtually identical. The energy of the singlet state is only ∼0.1 kcal/mol lower in energy than that of the triplet state and gives rise to the rather small calculated antiferromagnetic coupling constant of $J = -39$ cm^{-1}. Experimentally, a triplet ground state has been proposed based on the observation that the intensity of the triplet EPR signal of solid **10** increases with decreasing temperature (from 296 to 100 K). However, in this temperature range, the increase in the signal intensity with decreasing temperature is expected if the antiferromagnetic coupling constant is on the order of the calculated value even if the ground state is a singlet. A full variable-temperature (4−300 K) magnetochemical study is clearly called for. Nevertheless, it is evident that the singlet−triplet (or triplet−singlet) energy gap is small (<100 cm^{-1}) based on both the experimental and computational results.

2.11. Complex **11**. Geometry optimization of diamagnetic **11** was performed by a closed-shell singlet (RKS) calculation and a broken-symmetry BS(1,1) calculation. The latter was found to be 2.9 kcal/mol more stable than the RKS singlet solution (Figure 12a). The short C1−C1′ bond length of 1.428 Å [experimental value of 1.419(3) Å] of the coordinated bpy ligand indicates the presence of the π-radical anion $(bpy^{\bullet-})^-$.[38] All other C−C and C−N bond lengths also agree nicely with the experimental structure. The Mulliken spin-density plot shown in Figure 12a shows β-spin density (∼1e) located on the $(bpy^{\bullet-})^-$ ligand and α-spin density (∼1e) located on a low-spin Co^{II} ion (d^7, $S_{Co} = {}^1/_2$). The two spins are strongly antiferromagnetically coupled ($J = -2740$ cm^{-1}) and the spatial overlap integral S of the two magnetic orbitals is 0.63. Of the magnetic orbitals of **11**, the α-spin component is predominantly cobalt in character (75.5%) and the β-spin component is predominantly $(bpy^{\bullet-})^-$ in character (80.6%). The LUMO of **11** is a predominantly cobalt-centered σ-antibonding d orbital (61.5% cobalt). Complex **11** is, therefore, best described as $[(Cp^*)Co^{II}(bpy^{\bullet-})]^0$, a singlet diradical. Our calculations contrast the proposed electronic structure description of **11** as $[(\eta^5\text{-}Cp^*)Co^I(bpy^0)]^0$.[37]
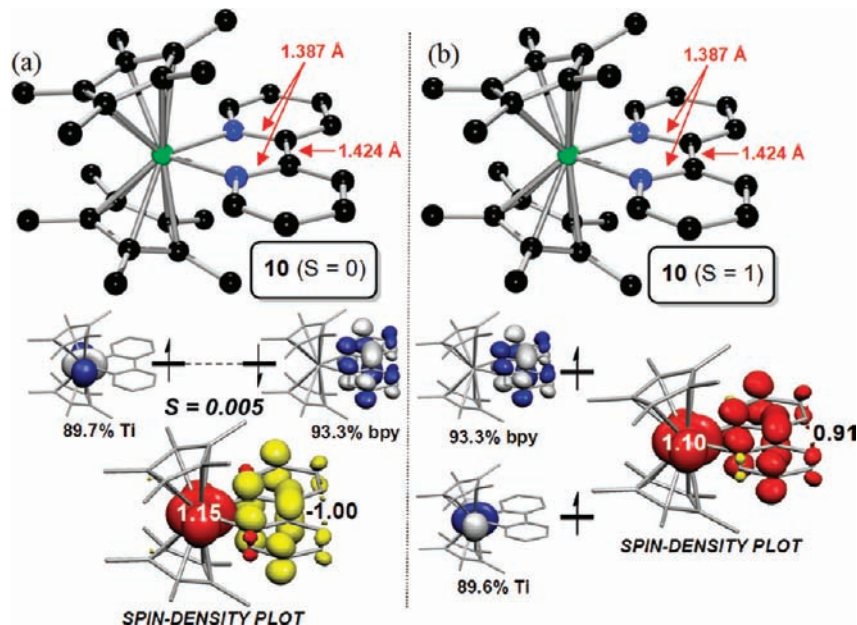

Figure 11. Calculated structure of **10** [(a) $S = 0$; (b) $S = 1$], with spin-density distribution (Mulliken) and frontier molecular orbital plots for both spin states. Color code: green, titanium; blue, nitrogen; black, carbon.
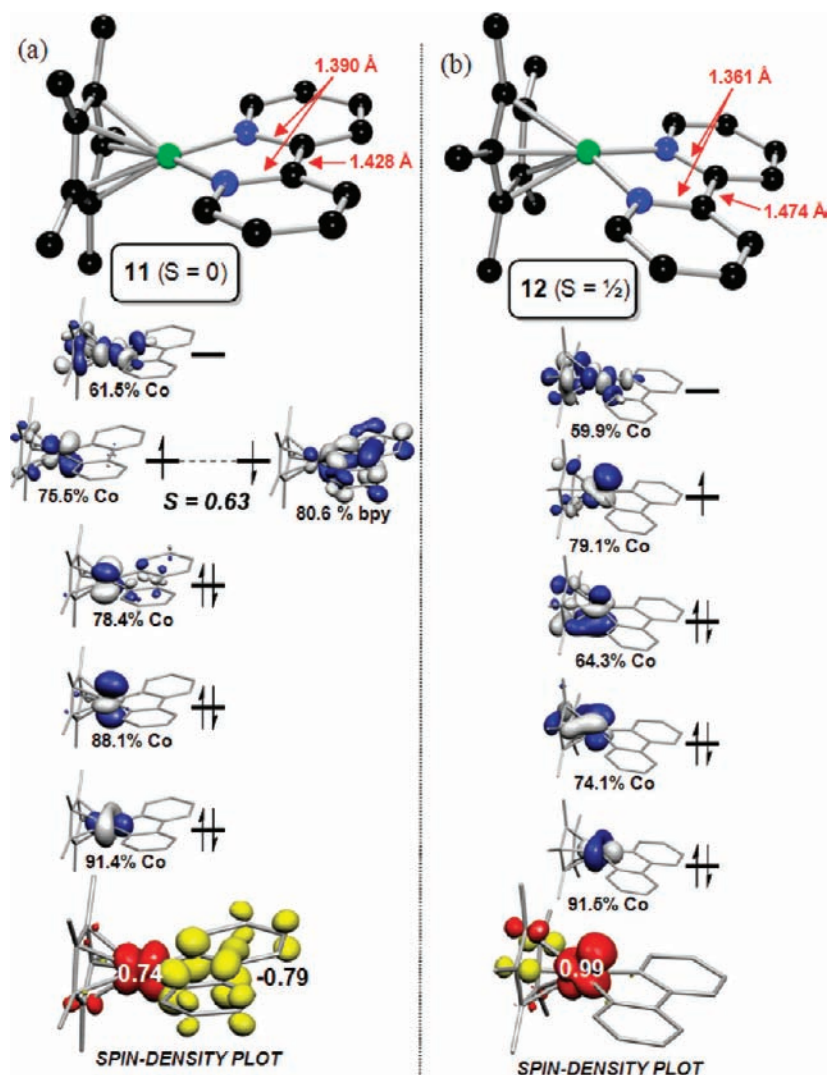
Figure 12. Calculated structures of (a) **11** ($S = 0$) and (b) **12** ($S = {}^1/_2$) and qualitative molecular orbital schemes and spin-density distributions (Mulliken). Color code: green, cobalt; blue, nitrogen; black, carbon.

DFT calculations (RKS) of the related compound $[(Cp^*)Rh(bpy)]^0$ have been reported;[47] our attempt to find a broken-symmetry solution for this species failed, and our calculations reproduced the results of ref 47. The electronic structure discrepancy between **11** and its Rh-containing congener $[(Cp^*)Rh(bpy)]^0$, namely, that **11** is a diradical and the rhodium species is not, highlights the important affect of both metal d-orbital energy and spatial distribution. In this case, $[(Cp^*)Rh(bpy)]^0$ is not a diradical because the rhodium d orbitals are large enough that high covalency establishes the closed-shell singlet electronic structure even though the HOMO contains nearly equivalent rhodium and bpy character (35.8% and 40.3%, respectively). The calculated C1—C1' bond length of 1.435 Å is consistent with the presence of a $(bpy^{\bullet-})^-$ radical monoanion; however, given the closed-shell singlet character of this species, we prefer the electronic structure description $[(Cp^*)Rh^{III}(bpy^{2-})]^0$, where substantial π donation from the $(bpy^{2-})^{2-}$ dianion to the Rh^{III} center is responsible for the calculated C1—C1' bond length.

*2.12. Complex **12***. Cation **12** is the one-electron-oxidized form of **11**; it possesses an $S = {}^1/_2$ ground state, but its structure is not known.[37] Geometry optimization (UKS) of the structure of the monocation **12** (Figure 12b) shows that, in agreement with the above calculations for **11**, the electron removed upon one-electron oxidation of **11** comes from the $(bpy^{\bullet-})^-$ π-radical anion to afford a neutral bpy^0 ligand in **12**, consistent with the long C1—C1' bond (1.474 Å) calculated for **12**. The unpaired electron resides in a cobalt-centered d orbital, as is observed by the experimental EPR spectrum (Co^{II}, d^7, $S = {}^1/_2$).[37]

*2.13. Complexes **13** and **14***. For complex **13**, namely, the monocation $[(\eta^5-Cp^*)Co^{III}(bpy^0)Cl]^+$ ($S = 0$), both a broken-symmetry and a closed-shell (RKS) calculation converged to the same closed-shell solution (Figure 13a). The geometrical features are summarized in Table 4. Note that no crystal structure of this species has been reported. The calculated bond distances in the N,N'-coordinated bpy ligand in **13** clearly show that it is present in its neutral form (bpy^0; calculated C1—C1' bond length of 1.473 Å). Therefore, the monocation **13** contains a central Co^{III} ion (d^6, $S_{Co} = 0$), an η^5-Cp^* monoanion, a chloride anion, and a neutral bpy^0 ligand: $[(\eta^5-Cp^*)Co^{III}(bpy^0)Cl]^+$.

We have also performed a UKS calculation on the neutral one-electron-reduced form of **13**, namely, $[(\eta^5-Cp^*)Co^{II}(bpy^0)Cl]^0$ (**14**, $S = {}^1/_2$). Experimental structural data have not been reported

9785

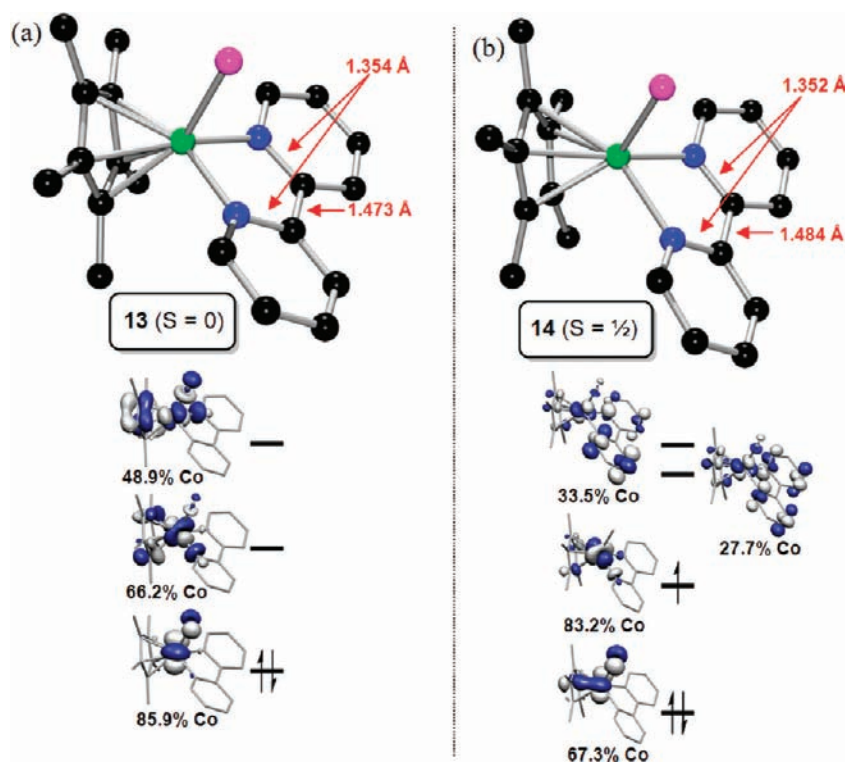dx.doi.org/10.1021/ic2005419 |*Inorg. Chem.* 2011, 50, 9773–9793

Figure 13. Calculated structures of (a) **13** ($S = 0$) and (b) **14** ($S = \frac{1}{2}$) and qualitative molecular orbital schemes. Color code: green, cobalt; pink, chlorine; blue, nitrogen; black, carbon.

for this compound.[37] The geometry-optimized structure (Figure 13b) shows that a neutral bpy^0 is present ($C1-C1'$ = 1.484 Å) and the SOMO is a metal-centered d orbital (83.2% cobalt). Thus, one-electron reduction of **13** is a predominantly metal-centered process. Experimentally, it has been shown that complex **14** rapidly loses a chloride ion in solution to afford complex **12**.

*2.14. Complex **15***. $[(toluene)Fe(bpy)]^0$ (**15**)[14] contains an η^6-bound neutral toluene ligand, possesses a diamagnetic ($S = 0$) ground state, and is isoelectronic to $[(\eta^5\text{-}Cp^*)Co^{II}(bpy^{\bullet-})]^0$ (**11**, $S = 0$). A geometry optimization of **15** starting from the experimental geometry has been carried out by a broken-symmetry $[BS(1,1)]$ calculation and a closed-shell singlet (RKS) calculation (Figure 14). It was found that the $BS(1,1)$ solution is 4.5 kcal/mol lower in energy than the closed-shell singlet solution. The N,N'-coordinated bpy ligand displays the geometrical features of a π-radical anion; the $C1-C1'$ bond length (1.418 Å) effectively reproduces the experimental value [1.417(3) Å]. The Mulliken spin-density plot shown in Figure 14 displays α-spin density (0.94e) on the metal ion and β-spin density (0.80e) located on the $(bpy^{\bullet-})^-$ ligand. The two spins are strongly antiferromagnetically coupled ($J = -2800$ cm^{-1}). The spatial overlap of the two magnetic orbitals is $S = 0.61$. The α-spin component of the "HOMO" in **15** is predominantly metal-centered (84.9% iron), and the β-spin component is predominantly $(bpy^{\bullet-})^-$-centered (86.0% bpy). Three doubly occupied metal-centered orbitals have also been identified, and the LUMO is predominantly an iron-centered (d-orbital) σ-antibonding orbital (69.8% iron), rendering the central ion as Fe^I (d^7, $S_{Fe} = \frac{1}{2}$). We have found no computational evidence for the "extensive π-backbonding to the 2,2'-bipyridine" from an Fe^0 center suggested in ref 14.

*2.15. Complex **16***. For the monoanion $[(\eta^5\text{-}Cp^*)Ru(bpy)]^-$ (**16**, $S = 0$), a closed-shell RKS geometry optimization yielded a structure that agrees very well with the crystallographically

determined structure described in ref 40 (Figure 15). Geometry optimization using broken-symmetry DFT provided the same molecular and electronic structure indicative of a closed-shell singlet species, which contrasts the electronic structure assignments of isoelectronic **11** and **15** as singlet diradicals. An η^5-coordinated cyclopentadienyl anion and a highly reduced bpy ligand are present in addition to a central ruthenium ion. Interestingly, the calculated $C1-C1'$ bond distance in **16** is very short (1.408 Å) and is in excellent agreement with the experimental values [1.413(9) and 1.401(9) Å for two crystallographically independent anions]. Similarly, the other calculated C—C and C—N bond distances in **16** are intermediate between those observed for an uncoordinated radical anion and a dianion.

We have identified three filled metal d orbitals (HOMO−1, HOMO−2, and HOMO−3) that possess 82.2%, 76.4%, and 85.9% ruthenium character (Figure 15). This is typical for a Ru^{II} ion with a low-spin d^6 configuration. The HOMO in **16** is of predominantly ligand character (72.7%) and represents a filled π^* orbital of bpy^0, rendering it an N,N'-coordinated *dianion* $(bpy^{2-})^{2-}$. This dianion undergoes some degree of π donation into an empty metal d orbital (ligand-to-metal donation). The HOMO possesses 17.3% ruthenium character (the remaining 10.0% is Cp^*-centered and is antibonding with respect to the ruthenium d orbital), and the Ru−N bonds are short and quite covalent. This explains the difference of the structural data of the $(bpy^{2-})^{2-}$ dianions in **16** and $[Al^{III}(bpy^{2-})_2]^-$ and $[Zr^{IV}(bpy^{2-})_3]^{2-}$ in refs 7 and 12, respectively. The electronic structure of **16** differs from those of isoelectronic **11** and **15** for two reasons: (1) the increased radial distribution of 4d compared to 3d orbitals provides a mechanism for higher overlap between the ruthenium d orbital and the bpy π^* orbital compared to the same interaction with an iron or cobalt d orbital and (2) the increased covalency of the second-row transition metals compared to first-row
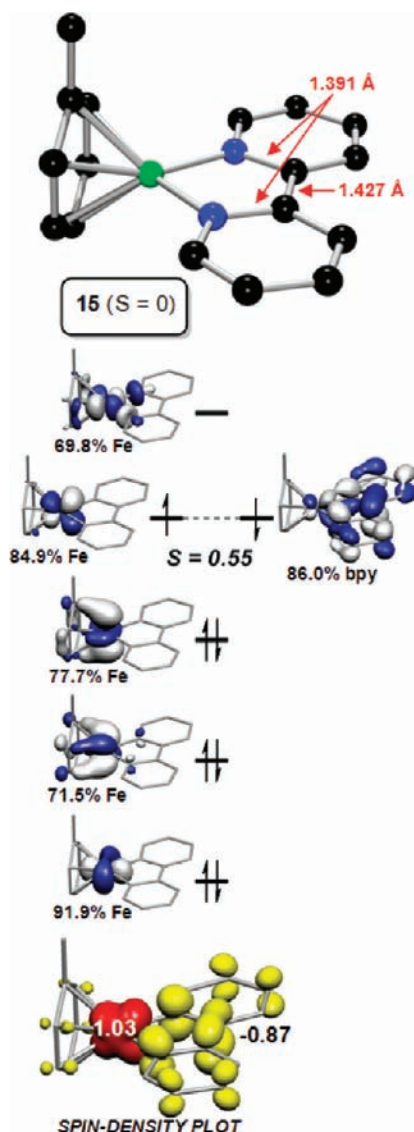
Figure 14. Calculated structure and qualitative molecular orbitals of **15**. Color code: green, iron; blue, nitrogen; black, carbon.
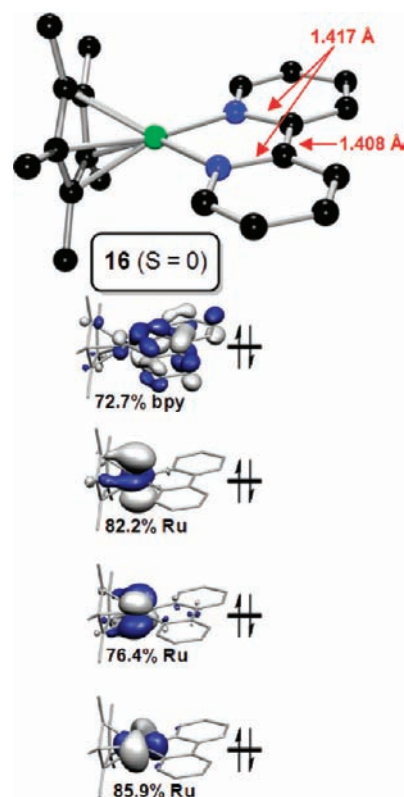

Figure 15. Calculated structure and qualitative molecular orbital diagram of **16**. Color code: green, ruthenium; blue, nitrogen; black, carbon.

with species **2**, **5**, **8**, **10**, and **17**, electronic structures of d^2/bpy^0 $(S_T = 0)$, $d^1/(bpy^{\bullet-})^-$ $(S_T = 0)$, and $d^0/(bpy^{2-})^{2-}$ $(S_T = 0)$ are all represented, highlighting the effect of the energy and spatial distribution of the metal d orbitals on the overall electronic structure.

We have also calculated the optimal geometry of a triplet excited state of **17**, which is 1.1 kcal/mol higher in energy than the closed-shell singlet state of **17**. We observe a half-filled zirconium d orbital (SOMO−1 is 79.0% ziconium) and a $(bpy^{\bullet-})^-$ π-radical anion (SOMO−2 is 92.8% bpy), indicating the electronic structure description $[(\eta^5\text{-Cp})Zr^{III}(bpy^{\bullet-})]^0$ $(S = 1)$. The structure of the Zr(bpy) unit is flat, as in the triplet states of **5**, **8**, and **10**.

*2.17. Complex **18***. A single-point broken-symmetry calculation $[BS(1,1)]$ on the crystal structure coordinates of **18** provided a solution that was nearly isoenergetic to (0.4 kcal/mol lower in energy than) the closed-shell singlet (RKS) solution that was reported in ref 42a (Figure 17). These nearly isoenergetic solutions indicate that a singlet diradical formulation for the electronic structure of **18** may be appropriate. This close energetic separation between the two solutions may also reflect complications associated with calculation of the energy of a monomeric unit of a polymeric crystal lattice. The best description of the electronic structure involves $[(CO)_3Mn^I$-$(bpy^{2-})]^-$ with significant π donation of the electron density from a $(bpy^{2-})^{2-}$ dianion to a Mn^I ion (d^6, $S_{Mn} = 0$). Overall, this π donation results in C1—C1$'$ and C—N distances resembling those of a $(bpy^{\bullet-})^-$ radical anion, which would imply the presence of Mn^0. The (bpy)Mn metallocycle exerts strong π backdonation into the carbonyl ligands: (bpy)Mn → CO.[42a] Thus, our calculations confirm those of Hartl et al.:[42a] the monoanion is probably best described as a compound with "fully delocalized π-bonding in the Mn(bpy) metallocycle and strong (bpy)Mn → CO π-backdonation".

transition metals suggests that the e$_g$ orbitals in **16** are substantially higher in energy than those in **11** and **15**, resulting in double occupation of the bpy π^* orbital in **16** being more favorable than an open-shell singlet derived from Ru^I antiferromagnetically coupled to a $(bpy^{\bullet-})^-$-centered radical anion.

*2.16. Complex **17***. The geometry-optimized structure (closed-shell, RKS) of $[(\eta^5\text{-Cp})_2Zr^{IV}(bpy^{2-})]^0$ (**17**) is shown in Figure 16. No broken-symmetry solution $[BS(1,1)]$ has been found for this species, in contrast to our calculations on isoelectronic **5**, **8**, and **10**. The calculated structure of **17** displays a strongly bent Zr(bpy) moiety $[\alpha(calcd) = 40.3°; \alpha(exptl)^{41} = 43.9°]$, and the C1—C1$'$ and C—N bond distances closely resemble those observed for an N,N$'$-coordinated dianion (Table 3). The HOMO of **17** (Figure 16) possesses 23.3% zirconium character and 71.9% bpy character. We, therefore, propose a dominant resonance structure $[(\eta^5\text{-Cp})Zr^{IV}$-$(bpy^{2-})]^0$ with strongly covalent Zr—N bonds due to π donation of the electron density from bpy^{2-} to the Zr^{IV} ion via bending of the average bpy plane away from that of the ZrN$_2$ plane. Note that this complex is isoelectronic with **2** $([(\eta^5\text{-Cp})_2V^{III}(bpy^0)]^+)$. Therefore,

Figure 16. Calculated structure and HOMO of **17**: (a) $S = 0$ ground state; (b) triplet excited state ($S = 1$). Color code: green, zirconium; blue, nitrogen; black, carbon).
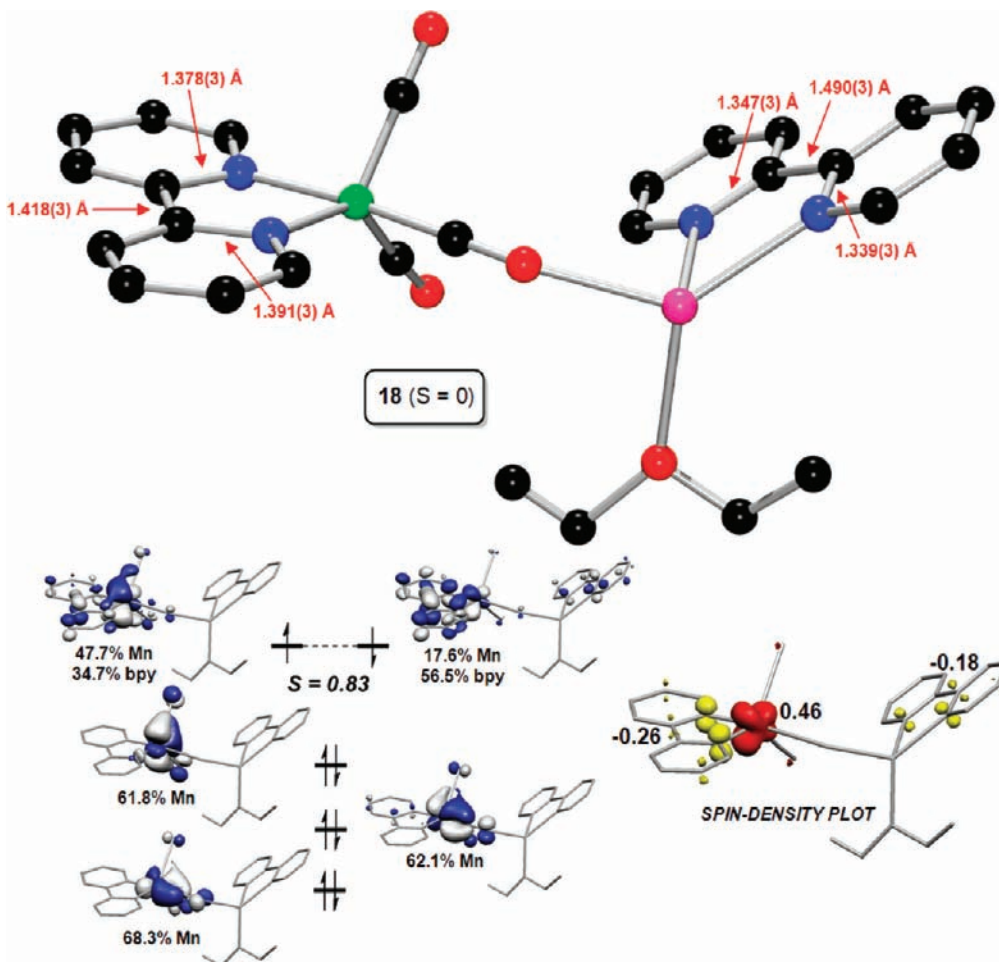
Figure 17. Calculated electronic structure using a broken-symmetry BS(1,1) approach for $[Na(bpy^0)(diethyl~ether)]^+[(CO)_3Mn^0(bpy^{\bullet-})]^-$ (**18**; single-point calculation on the crystal structure geometry), including a qualitative molecular orbital diagram and Mulliken spin-density distribution. Color code: green, manganese; pink, sodium; red, oxygen; blue, nitrogen; black, carbon.

These calculations suggest that metal-to-ligand π backdonation in $[(CO)_3Mn^{-I}(bpy^0)]^-$ plays only a minor (if any) role.

■ DISCUSSION

As summarized in Figure 1 and Tables 1 and 3, the most significant variation of the structural parameters of an N,N′-coordinated bpy-type ligand as a function of its oxidation level [neutral bpy^0, monoanionic π-radical $(bpy^{\bullet-})^-$, and dianion $(bpy^{2-})^{2-}$] is observed for the C1—C1′ bond and the two C1—N1 and C1′—N1′ bonds within the M(bpy) five-membered chelate ring. These bond lengths are almost always very similar to those reported for the free bpy^0 ligand and the sodium (potassium) salts of the monoanion and dianion.

In contrast to statements in the literature, the neutral ligand bpy^0 is only a week π acceptor (as has been quantified by its position in the spectrochemical series and the data in Table 2).[15,20] The C1—C1′, C1—N1, and C1′—N1′ bonds in complexes bearing bpy^0 are always very similar to those of the uncoordinated free ligand (see data in Table 3). π backdonation from the metal to the neutral bpy^0 ligand cannot play a significant role in the binding of a neutral bpy^0 ligand because, in general, the LUMO of the ligand is much higher in energy than the highest-filled metal d orbital (see data in Table 2).

The corresponding mono- and dianion, $(bpy^{\bullet-})^-$ and $(bpy^{2-})^{2-}$, have very weak or no π-acceptor character. In contrast, the dianion $(bpy^{2-})^{2-}$ can act as a fairly strong π donor because its HOMO has π symmetry and is, empirically, in the correct energy range for effective π donation.

The metal-to-nitrogen bond lengths are primarily governed by the σ-donor strength of the respective bpy^0, $(bpy^{\bullet-})^-$, and $(bpy^{2-})^{2-}$ ligands, which increases in this order because of the increasing electrostatic nature of the metal-to-ligand interaction. Only the $(bpy^{2-})^{2-}$ dianion will display an additional covalent π interaction with a suitable empty metal d orbital of π symmetry, leading to a further shortening of this bond.

It is therefore possible to unambiguously identify the neutral oxidation level of a bpy ligand in a given coordination complex by its rather uniform C1—C1′ distance at 1.47 ± 0.02 Å and its two C1—N1 and C1′—N1′ distances of 1.36 ± 0.01 Å (see Table 2). Any significant shortening of the C1—C1′ bond and, concomitantly, elongation of the C1—N1 and C1′—N1′ bonds is a clear indication for the reduction of the ligand by one or two electrons.

It is also now well established that the geometrical parameters of an N,N′-coordinated π-radical monoanion $(bpy^{\bullet-})^-$ are very similar to those observed for the corresponding sodium or potassium salts.[4a,b] In this form, the ligand is neither a good π acceptor nor a good π donor and, therefore, its geometrical parameters will not depend greatly on the nature of the transition-metal ion (or its d^n electron configuration) to which it is bound.

To the best of our knowledge, there are, to this date, only three crystallographically characterized (transition-)metal ion complexes containing a genuine dianionic $(bpy^{2-})^{2-}$ ligand, namely, $[Al^{III}(bpy^{2-})_2]^-$,[7] $[Zr^{IV}(bpy^{2-})_3]^{2-}$,[12] and **17**.[41c] The observed C1—C1′ distances at 1.36 ± 0.02 Å and the long C1—N1 and C1′—N1′ distances at 1.44 ± 0.02 Å are similar in these complexes and in the salt $[Na_2(bpy^{2-})(dme)_2]$.[5] It is conceivable that the dianion is a good π donor in coordination compounds with empty metal-centered π^* orbitals, as we have shown above for **16—18** and $[Cp^*Rh(bpy)]^0$. If sufficient electron density is shifted from the ligand dianion to the metal ion (π donation), the C—C and C—N bond lengths in the coordinated dianion can resemble those of a coordinated π-radical monoanion. A second consequence of this

mechanism is a shortening of the M—N bonds, giving it more covalent (double-bond) character. Thus, the crystallographically observed intraligand bond lengths of a monoanion can be obtained by two different mechanisms: (a) π donation of the electron density from the dianionic ligand to the metal ion or (b) a genuine π-radical monoanion that is coordinated to a metal ion via two M—N σ bonds. These two mechanisms can be identified and distinguished using DFT. If a broken-symmetry solution [e.g., BS(1,1)] for a diamagnetic molecule is significantly lower in energy than its closed-shell counterpart, a singlet diradical is likely to be the ground state. In a singlet diradical, the overlap integral S between the two magnetic orbitals (i.e., a metal d orbital and a ligand π^* orbital) is significantly less than 1.0 (antiferromagnetic coupling between the two magnetic orbitals). If, on the other hand, the ground state is a closed-shell singlet, the overlap integral S is expected to be 1.0 and the molecular orbital composed of a metal d orbital and a ligand π^* orbital is a HOMO filled with two electrons with antiparallel spins (Pauli principle).

In the following, we will discuss our computational results on the electronic structures of complexes **A**, **B**, and **1—18**. Complexes **A** and **B** both contain a central Sc^{III} ion with a d^0 configuration, which is the most stable oxidation state of scandium. The η^5-coordinated Cp* and $C_5H_4(CH_2)_2N(CH_3)_2$ ligands are closed-shell monoanions and, consequently, the bpy ligands in both **A** and **B** are π-radical monoanions $(bpy^{\bullet-})^-$. An intramolecular $\pi-\pi$ interaction of two $(bpy^{\bullet-})^-$ radicals in **A** yields a HOMO of π symmetry (Figure 2) that is filled by two electrons with antiparallel spins, allowing an $S = 0$ ground state. The HOMO possesses ~82% ligand character. This has been proposed by the original authors in ref 26 to explain the observed diamagnetism of **A** and is nicely corroborated by the present calculations. Interestingly, the calculated excited $S = 1$ state of **A** has a different structure than its singlet ground state counterpart: the $\pi-\pi$ interaction of the two $(bpy^{\bullet-})^-$ ligands is now disrupted by twisting the two bpy planes relative to each other.

In mononuclear **B**,[27] the two $(bpy^{\bullet-})^-$ radicals are coordinated in a cis configuration relative to each other (Figure 3b), which leads, via intramolecular antiferromagnetic coupling, to the observed singlet ground state and at slightly higher energy to the triplet excited state. Thus, **B** is a singlet diradical, where the BS(1,1) solution provides an overlap integral of $S = 0.32$. The experimental and calculated intraligand bond distances in **A** and **B** are in excellent agreement (Table 3), consistent with the notion that N,N′-coordinated $(bpy^{\bullet-})^-$ radical monoanions are present. Note that the triplet excited state of **B** has nearly the same geometric structure as the singlet ground-state structure. The calculated energy difference between the singlet and triplet states of ~600 cm^{-1} (based on a calculated coupling constant $J = -293$ cm^{-1}, $H = -2J \cdot \vec{S}_1 \cdot \vec{S}_2$, and $S_1 = S_2 = \frac{1}{2}$) agrees well with the experimentally determined small paramagnetism of **B** at ambient temperature. A full variable-temperature study of the magnetic susceptibility of solid **B** could verify the calculations quantitatively.

It is gratifying that the computational methodology that we have employed successfully reproduces the experimental structural and electronic structural data of **A** and **B**, including subtle effects such as $\pi-\pi$ interactions in **A** and ferromagnetic as well as antiferromagnetic spin-coupling phenomena of two cis-configured π-radical anions $(bpy^{\bullet-})^-$ in **B**. These results encouraged us to use this methodology with confidence in cases where the oxidation state of the central metal ion is not restricted to one very stable form, such as, for example, Sc^{III} in **A** and **B**.

The electron-transfer series consisting of the vanadium complexes **1**−**3**, the structures of which are shown in Figures 4 and 5, is interesting in that the two Cp^- monoanions in **1** are coordinated in an η^5 fashion and another one in an η^3 fashion (ring slippage), whereas in **2** and **3**, both Cp^- ligands are coordinated in an η^5 fashion. This structural feature of neutral **1**[28b] is nicely reproduced in the calculations, which show an energetically low-lying solution where a central V^{III} ion (d^2, $S_V = 1$) is antiferromagnetically coupled to a π-radical anion $(bpy^{\bullet-})^-$, yielding the observed $S = {}^1/_2$ ground state: $[(\eta^5\text{-}Cp)(\eta^3\text{-}Cp)V^{III}(bpy^{\bullet-})]^0$ $(S = {}^1/_2)$.
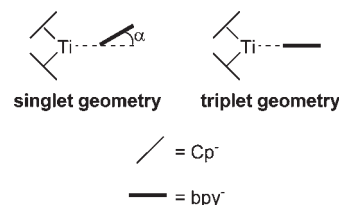
One-electron oxidation of **1** to **2** is a ligand-centered process that is accompanied by a rearrangement of the η^3-bound Cp^- in **1** to an η^5-bound Cp^- in diamagnetic **2**. A closed-shell calculation of **2** reproduces the experimental structure,[28b] and a broken-symmetry $[BS(1,1)]$ calculation converged to the same solution. The HOMO in **2** is a doubly occupied metal d orbital (∼84% vanadium), rendering the central vanadium ion as low-spin V^{III}. The transformation from **1** to **2** is complicated: oxidation of **1** occurs at a ligand-centered orbital and results in a change of spin state at the metal from high-spin d^2 in **1** (which favors ring slippage) to low-spin d^2 in **2** (which does not favor ring slippage). Apparently, antiferromagnetic coupling between the $(bpy^{\bullet-})^-$ radical monoanion and the high-spin V^{III} center in **1** provides the stabilization required to overcome the destabilization associated with population of a V−Cp antibonding orbital, the occupation of which results in $\eta^5 \rightarrow \eta^3$ ring slippage. The corresponding calculated triplet excited state of **2** (quite close in energy to the singlet) is achieved only if one Cp^- undergoes $\eta^5 \rightarrow \eta^3$ ring slippage. The two SOMOs of triplet **2** are metal-centered (93% and 79%, respectively), rendering the central vanadium ion a V^{III} (d^2, $S = 1$) species. The bpy ligand in **2** ($S = 1$) is clearly a neutral ligand. Considering these computational results for the monocation **2**, we feel that it would be important to spectroscopically investigate the electronic structure of **2** in more detail.

A further one-electron oxidation of the monocation **2** to the dication **3** is a metal-centered process ($V^{III} \rightarrow V^{IV}$), and the calculated structure of **3** displays two η^5-Cp^- anions and a neutral bpy^0 ligand. The SOMO in **3** possesses ∼93% metal d character. This is in excellent agreement with the EPR spectroscopic results.[29] Thus, the above calculations reproduce all known spectroscopic and structural features of the electron-transfer series **1**−**3** very reliably:

$$[(\eta^5\text{-}Cp)(\eta^3\text{-}Cp)V^{III}(bpy^{\bullet-})]^0 \underset{+\,e}{\overset{-\,e}{\rightleftarrows}} [(\eta^5\text{-}Cp)_2V^{III}(bpy^0)]^{1+}$$
1 $(S = {}^1/_2)$ **2** $(S = 0)$

$$+\,e \big\Vert -\,e$$

$$[(\eta^5\text{-}Cp)_2V^{IV}(bpy^0)]^{2+}$$
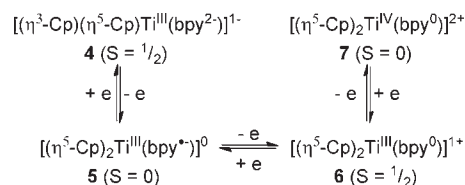**3** $(S = {}^1/_2)$
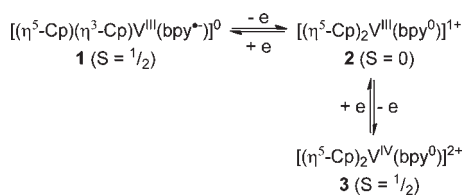
In a similar fashion, we have also computationally studied the four-membered electron-transfer series **4**−**7** shown in Figures 6−8. We have established that **5** contains a central Ti^{III} ion, two Cp^- anions, and a π-radical monoanion $(bpy^{\bullet-})^-$. **5** possesses a singlet ground state that is attained via intramolecular antiferromagnetic coupling of the spins of the Ti^{III} ion (d^1) and the π-radical monoanion $(bpy^{\bullet-})^-$ (Figure 7). A BS(1,1) solution has been found. The calculated singlet−triplet energy gap in **5** is small and in good agreement with experiment. The presence of a bent Ti(bpy) unit in the singlet state has been reproduced computationally. The optimized geometry of the
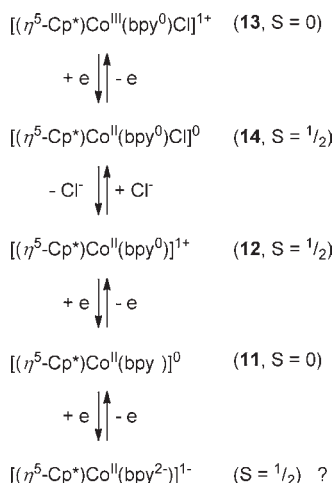
triplet excited state of the $Ti^{III}(bpy^{\bullet-})$ moiety is now flat. These features have been correctly proposed by the original authors in 1978.[30a] One-electron oxidation of **5** to **6** is a ligand-based process, whereas **6** to **7** (Figure 7) is metal-centered. The one-electron reduction of **5** to **4** is a ligand-centered process.

$$[(\eta^3\text{-}Cp)(\eta^5\text{-}Cp)Ti^{III}(bpy^{2-})]^{1-} \qquad [(\eta^5\text{-}Cp)_2Ti^{IV}(bpy^0)]^{2+}$$
4 $(S = {}^1/_2)$ **7** $(S = 0)$

$$+\,e \big\Vert -\,e \qquad\qquad -\,e \big\Vert +\,e$$

$$[(\eta^5\text{-}Cp)_2Ti^{III}(bpy^{\bullet-})]^0 \underset{+\,e}{\overset{-\,e}{\rightleftarrows}} [(\eta^5\text{-}Cp)_2Ti^{III}(bpy^0)]^{1+}$$
5 $(S = 0)$ **6** $(S = {}^1/_2)$

The electronic structures of the neutral complexes **5** (Figure 7), **8**, (Figure 9), and **10** (Figure 11) allow some interesting observations to be made:[30,31] the $Ti^{III}(bpy^{\bullet-})$ or $Ti^{III}(biquinoline^{\bullet-})$ moieties are flat in **8** and **10** but bent in **5** in the singlet state; all three species possess such flat moieties in the triplet excited state. The bonding in the singlet state allows an antiferromagnetic coupling between the spins of a metal-centered d^1 orbital and a bpy-centered π^{*1} orbital, the magnitude of which increases with increasing bending angle α (Scheme 3). In flat Ti(L) moieties, the overlap integral S becomes very small (approaching zero), with the consequence that the triplet state is stabilized to the degree where, computationally, the singlet and triplet states are nearly degenerate. It is unfortunate that, at present, these predictions cannot be validated because of a lack of pertinent experimental data in refs 31 and 33, although it has been proposed that **10** possesses a triplet ground state (EPR spectroscopy),[31] whereas **5** is diamagnetic. The spin state of **7** has not been reported,[33] but the fact that it is paramagnetic $[1.62\ \mu_B$ at ambient (?) temperature] may indicate a singlet−triplet equilibrium, which would be in excellent agreement with the present calculations. More magnetochemical and other spectroscopic data on **5**, **8**, and **10** are needed in order to validate our present DFT models for these complexes.

In the context of compounds **5**, **8**, and **10**, the zirconium complex **17** (Figure 16) is of interest because it is formally isoelectronic with **5**, **8**, and **10**, although the zirconium 4d orbitals are larger than those of the corresponding 3d orbitals in **5**, **8**, and **10**. The calculated closed-shell structure of **17** displays a larger bending angle α in **17** than in **5**. Consequently, the HOMO of **17** shown in Figure 16 possesses ∼23% zirconium and ∼73% bpy character; it is not a singlet diradical because a BS(1,1) calculation converged on the same result as this RKS calculation. A description of its electronic structure as $[(\eta^5\text{-}Cp)_2Zr^{IV}(bpy^{2-})]$ with significant π donation from the $(bpy^{2-})^{2-}$ ligand to the Zr^{IV} ion affords structural features that approach those characteristic for a coordinated π-radical anion $(bpy^{\bullet-})^-$. The Mulliken spin population analysis shows zero spin density at the central zirconium ion and at the ligand, contrasting the

Scheme 4

$$[(\eta^5\text{-Cp*})\text{Co}^{III}(\text{bpy}^0)\text{Cl}]^{1+} \quad (\textbf{13}, S = 0)$$

$$+ e \big\updownarrow - e$$

$$[(\eta^5\text{-Cp*})\text{Co}^{II}(\text{bpy}^0)\text{Cl}]^0 \quad (\textbf{14}, S = {}^1/_2)$$

$$- \text{Cl}^- \big\updownarrow + \text{Cl}^-$$

$$[(\eta^5\text{-Cp*})\text{Co}^{II}(\text{bpy}^0)]^{1+} \quad (\textbf{12}, S = {}^1/_2)$$

$$+ e \big\updownarrow - e$$

$$[(\eta^5\text{-Cp*})\text{Co}^{II}(\text{bpy}^{\bullet-})]^0 \quad (\textbf{11}, S = 0)$$

$$+ e \big\updownarrow - e$$

$$[(\eta^5\text{-Cp*})\text{Co}^{II}(\text{bpy}^{2-})]^{1-} \quad (S = {}^1/_2) \ ?$$

electronic structures of **5**, **8**, and **10** (Figures 7, 9, and 11), which are singlet diradicals. We have found no computational evidence for a d^2 electron configuration at the central zirconium ion and an electronic structure description as $[(\eta^5\text{-Cp})_2\text{Zr}^{II}(\text{bpy}^0)]^0$ with strong metal-to-ligand π backdonation, as was suggested in ref 41c. Interestingly, the first triplet excited state corresponds to the description $[(\eta^5\text{-Cp})_2\text{Zr}^{III}(\text{bpy}^{\bullet-})]^0$ ($S = 1$), which is a clear indication of the inherent stability of the Zr^{IV} ion (d^0) over Zr^{III} or Zr^{II}.

The cobalt complexes **11** and **12** possess electronic structures that are best described as $[(\eta^5\text{-Cp*})\text{Co}^{II}(\text{bpy}^{\bullet-})]^0$ ($S = 0$) and $[(\eta^5\text{-Cp*})\text{Co}^{II}(\text{bpy}^0)]^+$ ($S = {}^1/_2$) according to the present DFT calculations (Scheme 4). This one-electron oxidation of **11** to **12** is a ligand-centered process: $(\text{bpy}^{\bullet-})^- \rightarrow \text{bpy}^0$. The addition of a chloride ion to the monocation **12** yields complex **14**, which displays the electronic structure $[(\eta^5\text{-Cp*})\text{Co}^{II}\text{Cl}(\text{bpy}^0)]^0$ ($S = {}^1/_2$). One-electron oxidation of **14** yields **13**, a Co^{III} species best described as $[(\eta^5\text{-Cp*})\text{Co}^{III}\text{Cl}(\text{bpy}^0)]^+$; the one-electron oxidation of **14** to **13** is, therefore, a metal-centered process.

Isoelectronic **11** and **15** are both singlet diradicals: $[(\eta^5\text{-Cp*})\text{Co}^{II}(\text{bpy}^{\bullet-})]^0$ ($S = 0$) and $[(\eta^6\text{-toluene})\text{Fe}^{I}(\text{bpy}^{\bullet-})]^0$ ($S = 0$), respectively. **15** has originally been described as Fe^0, although "a substantial transfer of electron density from the iron atom to the π^* orbitals of bipyridine" has been proposed. This mechanism and the corresponding electronic structure are not correct. The BS(1,1) computational solution for **15** points to a singlet diradical, where an Fe^I central ion (d^7, $S_{\text{Fe}} = {}^1/_2$) couples antiferromagnetically to a $(\text{bpy}^{\bullet-})^-$ radical anion. Isoelectronic complex **16**, on the other hand, should be described as $[(\eta^5\text{-Cp*})\text{Ru}^{II}(\text{bpy}^{2-})]^-$ ($S = 0$). Complexes **11**, **15**, and **16** are isoelectronic, but their intramolecular electron density distributions differ: **11** is d^7 (low-spin) $(\text{bpy}^{\bullet-})^-$; **15** is d^7 (low-spin) $(\text{bpy}^{\bullet-})^-$; **16** is d^6 (low-spin) $(\text{bpy}^{2-})^{2-}$. In **16**, an N,N'-coordinated $(\text{bpy}^{2-})^{2-}$ dianion transfers electron density to the central ruthenium ion via ligand-to-metal π donation, giving it some reduced Ru^{II} character and some oxidized character of the $(\text{bpy}^{2-})^{2-}$ anion.

■ CONCLUSIONS

In this paper, we have laid out what we consider to be guiding principles for the assignment of the oxidation level of bpy in a given coordination compound. On the basis of the $C1-C1'$

bond length alone, a neutral bpy^0 ligand can be identified if this bond length is within the range 1.47 ± 0.02 Å. This is because bpy^0 is a *very* weak π acceptor, so weak, in fact, that structural distortions of the intraligand bond lengths of bpy^0 associated with π backdonation from a transition-metal ion into the bpy-centered LUMO are not observable by X-ray crystallography. Similarly, the presence of a $(\text{bpy}^{2-})^{2-}$ dianion can be unambiguously assigned based on the $C1-C1'$ bond length if it falls within the range 1.36 ± 0.02 Å. The assignment of a given bpy oxidation level becomes more complicated when the $C1-C1'$ bond length is intermediate. On the basis of empirical observations and DFT calculations, we propose here that $(\text{bpy}^{2-})^{2-}$ may act as a strong π donor, giving $C1-C1'$ bond lengths that range between that observed for the π-radical monoanion $(\text{bpy}^{\bullet-})^-$ (~1.43 Å) and that observed for the $(\text{bpy}^{2-})^{2-}$ dianion in the absence of a π-accepting metal ion (~1.36 Å). Differentiation between the following two electronic structure descriptions is not possible based on structural data alone: (a) (bpy^{2-})M with strong π donation from the $(\text{bpy}^{2-})^{2-}$ dianion to the metal ion and (b) a $(\text{bpy}^{\bullet-})^-$ radical monoanion antiferromagnetically coupled to a transition-metal ion. Differentiation between these two bonding modes requires a more in-depth spectroscopic and variable-temperature magnetochemical investigation and may be aided by broken-symmetry DFT calculations. Ideally, electronic structures derived from DFT calculations would be verified by calculating measurable spectroscopic and structural parameters in order to justify the electronic structure assignment. Despite the difficulties of differentiating between electronic structure descriptions (a) and (b), the following guiding principles may allow one to a priori assign a bpy ligand oxidation level with some confidence, although the assignment should be verified by experiment and/or theory. First, the radial distribution of 3d orbitals is smaller than the corresponding distribution in 4d and 5d orbitals, and a diradical description [i.e., $(\text{bpy}^{\bullet-})^-$ antiferromagnetically coupled to a transition-metal ion] is generally favored with first-row transition metals, whereas a description involving π donation from a $(\text{bpy}^{2-})^{2-}$ dianion to a transition-metal ion is more common with second- and third-row transition metals. Second, and more subtly, the geometry of a particular species may have a profound impact on the electronic structure description, wherein geometries involving weak spatial overlap between metal-centered d orbitals and the bpy π^* LUMO favor a diradical formulation, whereas geometries that provide a mechanism for increased overlap between these orbitals may favor a π-donation model. Finally, the relative energies of metal d orbitals and the bpy π^* LUMO must be closely matched for a diradical electronic structure description to be valid, and calibration to this variable requires exposure to a broad array of compounds such as that presented in this manuscript.

In conclusion, bpy^0 is a *very* weak π acceptor,[15,20] $(\text{bpy}^{\bullet-})^-$ is neither a π donor nor a π acceptor but is ideally suited for a productive antiferromagnetic coupling interaction with an open-shell transition-metal ion, and $(\text{bpy}^{2-})^{2-}$ may be a strong π donor. Differentiation between these descriptions requires a combination of theory and experiment, as has been described in this manuscript.

■ EXPERIMENTAL SECTION

All DFT calculations were performed using the *ORCA* program package.[48] $[(\text{Cp})_2\text{Ti}^{III}(\text{bpy}^{\bullet-})]^0$ (**5**) is the most well-characterized diradical described in this paper, with known geometry from an X-ray

crystal structure[31a] and a measured antiferromagnetic exchange-coupling constant, J, of approximately -300 cm^{-1}.[30] We have calculated this species using four functionals, namely, BP86,[49] B3LYP,[50−52] TPSS,[53] and TPSSh.[54] The best agreement between the measured and calculated antiferromagnetic exchange-coupling constants for **5** was obtained with the B3LYP functional (see the Supporting Information), and the known geometry of this species was also satisfactorily reproduced. Therefore, we have carried out all calculations reported in this manuscript (geometry optimizations and single-point calculations for complexes **A**, **B**, **1−18**, and $[Cp^*Rh(bpy)]^0$) using this functional.

The all-electron Gaussian basis sets were those developed by the Ahlrichs group.[51,52] All calculations have been performed using an empirical van der Waals correction to the DFT energy.[57] For metal and other atoms directly coordinated to a metal (including the carbon atoms of cyclopentadienyl rings), triple-ζ quality basis sets (TZVP) with one set of polarization functions were employed (see the Supporting Information for results with other basis sets).[56] For all atoms not bound directly to a metal, slightly smaller polarized split-valence SV(P) basis sets were employed that were double-ζ quality in the valence region and contained a polarizing set of d functions on the non-hydrogen atoms.[55] Auxiliary basis sets used to expand the electron density in the resolution-of-the-identity (RI) approach were chosen[58−60] to match the orbital basis. For compounds **17** and **18**, which include second-row transition-metal ions, the zeroth-order regular approximation (ZORA) method[57] was implemented; in these calculations, ZORA-TZVP[58] and ZORA-SV(P)[62] replaced the standard basis sets TZVP and SV(P), respectively. The radial integration accuracy for all calculations was improved by setting the radial resolution parameters to 10 for all metals and 5 for all other atoms.

The self-consistent-field calculations were tightly converged (1×10^{-8} E$_h$ in energy, 1×10^{-7} E$_h$ in density change, and 1×10^{-7} in the maximum element of the DIIS error vector). All geometries were tightly optimized and were carried out in redundant internal coordinates without imposing symmetry constraints. Geometry optimization was considered converged after the energy change was less than 1×10^{-6} E$_h$, the gradient norm and maximum gradient element were smaller than 3×10^{-5} and 1×10^{-4} E$_h$ bohr^{-1}, respectively, and the root-mean-square and maximum displacements of all atoms were smaller than 6×10^{-4} and 1×10^{-3} bohr, respectively.

Throughout this paper, we describe our computational results by using the broken-symmetry (BS) approach described by Ginsberg[59] and Noodleman.[60] Because several BS solutions to the spin UKS equations may be obtained, the general notation BS(m,n)[61] has been adopted, where m (n) denotes the number of spin-up (spin-down) electrons at the two interacting fragments. Unrestricted corresponding orbitals,[62] quasi-restricted orbitals,[63] and canonical orbitals (isoelectron density surfaces = 95%) as well as spin-density plots (isoelectron density surfaces = 99.5%) were generated with the program *Molekel*, version 4.3.[64−68]

ASSOCIATED CONTENT

S **Supporting Information.** Geometry-optimized molecular *xyz* coordinates for complexes **A**, **B**, **1−17**, and $[(Cp^*)Rh-(bpy)]^0$; comparison of DFT calculations and basis sets in calculating **5**; comparisons between optimized and experimental structures; a comparison of the electronic structures for these compounds derived from single-point calculations on crystal structure geometries (where available) and geometry optimizations; absolute energies; atomic charge and spin-density distributions; and Mulliken, Loewdin, and natural population analyses for members of the electron-transfer series $[(Cp)_2Ti(bpy)]^{2+/+/0/-}$ (**4−7**). This material is available free of charge via the Internet at http://pubs.acs.org.

AUTHOR INFORMATION

Corresponding Author
*E-mail: wieghardt@mpi-muelheim.mpg.de.

ACKNOWLEDGMENT

REFERENCES

(1) The coordination chemistry of the bpy ligand with transition-metal ions has been comprehensively reviewed up to 1989: Constable, E. C. *Adv. Inorg. Chem.* **1989**, *34*, 1−37.

(2) In this paper, we will use the abbreviation bpy in a generic sense; i.e., in these cases, we do not wish to assign a specific oxidation level of the ligand. In contrast, we will use bpy^0 to indicate the presence of a neutral ligand, $(bpy^{\bullet-})^-$ for the π-radical monoanion and $(bpy^{2-})^{2-}$ for the diamagnetic dianion.

(3) Chisholm, M. H.; Huffman, J. C.; Rothwell, I. P.; Bradley, P. G.; Kress, N.; Woodruff, W. H. *J. Am. Chem. Soc.* **1981**, *103*, 4945−4947.

(4) (a) Gore-Randall, E.; Irwin, M.; Denning, M. S.; Goicoechea, J. M. *Inorg. Chem.* **2009**, *48*, 8304−8316. (b) Echegoyen, L.; DeCian, A.; Fischer, J.; Lehn, J.-M. *Angew. Chem., Int. Ed. Engl.* **1991**, *30*, 838−840.

(5) Bock, H.; Lehn, J.-M.; Pauls, J.; Holl, S.; Krenzel, V. *Angew. Chem., Int. Ed.* **1999**, *38*, 952−955.

(6) Bellavance, P. L.; Corey, E. R.; Corey, J. Y.; Hey, G. W. *Inorg. Chem.* **1977**, *16*, 462−467.

(7) Nikiforov, G. B.; Roesky, H. W.; Noltemeyer, M.; Schmidt, H.-G. *Polyhedron* **2004**, *23*, 561−566.

(8) Irwin, M.; Jenkins, R. K.; Denning, M. S.; Krämer, T.; Grandjean, F.; Long, G. J.; Herchel, R.; McGrady, J. E.; Goicoechea, J. M. *Inorg. Chem.* **2010**, *49*, 6160−6171.

(9) $[La^{III}(Tp^{Me2})_2(bpy^{\bullet-})]^0$ $[S = ^1/_2;$ Tp* = hydrotris(3,5-dimethylpyrazolyl)borate(1−)]: Roitershtein, D.; Domingos, Â.; Pereira, L. C. J.; Ascenso, J. R.; Marques, N. *Inorg. Chem.* **2003**, *42*, 7666−7673.

(10) $[(Cp^*)_2Sm^{III}(bpy^{\bullet-})]^0$: (a) Evans, W. J.; Drummond, D. K. *J. Am. Chem. Soc.* **1989**, *111*, 3329−3335. $[(Cp^*)_2Yb^{III}(bpy^{\bullet-})]^0$: (b) Schultz, M.; Boncella, J. M.; Berg, D. J.; Tilley, T. D.; Andersen, R. A. *Organometallics* **2001**, *21*, 460−472.

(11) $[(Tp^*)_2U^{III}(bpy^{\bullet-})]^0$ and $[(Tp^*)_2U^{III}I_2(bpy^0)]^0$: Kraft, S. J.; Fanwick, P. E.; Bart, S. C. *Inorg. Chem.* **2010**, *49*, 1103−1110.

(12) Rosa, P.; Mézailles, N.; Ricard, L.; Mathey, F.; Le Floch, P. *Angew. Chem., Int. Ed.* **2000**, *39*, 1823−1826.

(13) (a) Lentz, M. R.; Fanwick, P. E.; Rothwell, I. P. *Organometallics* **2003**, *22*, 2259−2266. (b) Chisholm, M. H.; Kober, E. M.; Ironmonger, D. J.; Thornton, P. *Polyhedron* **1985**, *4*, 1869−1874.

(14) Radonovich, L. J.; Eyring, M. W.; Groshens, T. J.; Klabunde, K. J. *J. Am. Chem. Soc.* **1982**, *104*, 2816−2819.

(15) Tom Dieck, H.; Franz, K.-D.; Hohmann, F. *Chem. Ber.* **1975**, *108*, 163−173.

(16) (a) $[Fe^{II}(bpy^0)_3]^{2+}$ ($S = 0$): Batten, S. R.; Murray, K. S.; Sinclair, N. J. *Acta Crystallogr., Sect. C: Cryst. Struct. Commun.* **2000**, *C56*, E320−E320. (b) $[Ru^{II}(bpy^0)_3]^{2+}$ ($S = 0$): Biner, M.; Bürgi, H. B.; Ludi, A.; Röhr, C. *J. Am. Chem. Soc.* **1992**, *114*, 5197−5203. (c) $[Os^{II}(bpy^0)_3]^{2+}$ ($S = 0$): Constable, E. C.; Raithby, P. R.; Smit, D. N. *Polyhedron* **1989**, *8*, 367−369.

(17) (a) $[Co^{III}(bpy^0)_3]^{3+}$ ($S = 0$): Jun, Q.; Zhang, C. *Acta Crystallogr., Sect. E: Struct. Rep. Online* **2010**, *E66*, m12. (b) $[Rh^{III}(bpy^0)_3]^{3+}$ ($S = 0$): Hubesch, B.; Mahieu, B.; Meunierpiret, J. *Bull. Chim. Belg.* **1985**, *94*, 685−695. (c) $[Ir^{II}(bpy^0)_3]^{3+}$ ($S = 0$): Hazell, A. C.; Hazell, R. G. *Acta Crystallogr., Sect. C: Cryst. Struct. Commun.* **1984**, *C40*, 806−811.

(18) Goodwin, K. V.; Pennington, W. T.; Petersen, J. D. *Inorg. Chem.* **1989**, *28*, 2016−2018.

(19) Baker, R. J.; Jones, C.; Kloth, M.; Mills, D. P. *New J. Chem.* **2004**, *28*, 207−213.

(20) (a) Josephsen, J.; Schäffer, C. E. *Acta Chem. Scand. A* **1977**, *31*, 813–824. (b) Hancock, R. D.; McDougall, G. J. *J. Chem. Soc., Dalton Trans.* **1977**, 67–70.

(21) (a) Hieber, W.; Mühlbauer, F. *Z. Anorg. Allg. Chem.* **1935**, *221*, 337–348. (b) Hieber, W.; Romberg, E. *Z. Anorg. Allg. Chem.* **1935**, *221*, 349–353. (c) Stiddard, M. H. B. *J. Chem. Soc.* **1962**, 4712–4715.

(22) Le Floch, P.; Carmichael, D.; Ricard, L.; Mathey, F.; Jutand, A.; Amatore, C. *Organometallics* **1992**, *11*, 2475–2479.

(23) (a) Kaizu, Y.; Kobayashi, H. *Bull. Chem. Soc. Jpn.* **1970**, *43*, 2492–2494. (b) Kaizu, Y.; Kobayashi, H. *Bull. Chem. Soc. Jpn.* **1972**, *45*, 470–477. (c) Vlček, J. A.; Baumann, F.; Kaim, W.; Grevels, F.-W.; Hartl, F. *J. Chem. Soc., Dalton Trans.* **1998**, 215–220.

(24) Záliš, S.; Daniel, C.; Vlček, A. *J. Chem. Soc., Dalton Trans.* **1999**, 3081–3086.

(25) (a) Farrell, I. R.; Hartl, F.; Zalis, S.; Wanner, M.; Kaim, W.; Vlček, A. *Inorg. Chim. Acta* **2001**, *318*, 143–151. (b) Farrell, I. R.; Hartl, F.; Záliš, S.; Mahabiersing, T.; Vlček, A., Jr. *J. Chem. Soc., Dalton Trans.* **2000**, 4323–4331.

(26) Tupper, K. A.; Tilley, T. D. *J. Organomet. Chem.* **2005**, *690*, 1689–1698.

(27) Beetstra, D. J.; Meetsma, A.; Hessen, B.; Teuben, J. H. *Organometallics* **2003**, *22*, 4372–4374.

(28) (a) Fachinetti, G.; Del Nero, S.; Floriani, C. *J. Chem. Soc., Dalton Trans.* **1976**, 1046–1049. (b) Jordan, M.; Saak, W.; Haase, D.; Beckhaus, R. *Eur. J. Inorg. Chem.* **2007**, 5168–5172.

(29) Ghosh, P.; Kotchevar, A. T.; DuMez, D. D.; Ghosh, S.; Peiterson, J.; Uckun, F. M. *Inorg. Chem.* **1999**, *38*, 3730–3737.

(30) (a) McPherson, A. M.; Fieselmann, B. F.; Lichtenberger, D. L.; McPherson, G. L.; Stucky, G. D. *J. Am. Chem. Soc.* **1979**, *101*, 3425–3430. (b) Bishop, L. A.; Turner, M. A.; Kool, L. B. *J. Organomet. Chem.* **1998**, *553*, 53–57.

(31) (a) Gyepes, R.; Witte, P. T.; Horáček, M.; Císařová, I.; Mach, K. *J. Organomet. Chem.* **1998**, *551*, 207–213. (b) Witte, P. T.; Klein, R.; Kooijman, H.; Spek, A. L.; Polášek, M.; Varga, V.; Mach, K. *J. Organomet. Chem.* **1996**, *519*, 195–204.

(32) Thewalt, U.; Berhalter, K. *J. Organomet. Chem.* **1986**, *302*, 193–200.

(33) Piglosiewicz, I. M.; Beckhaus, R.; Saak, W.; Haase, D. *J. Am. Chem. Soc.* **2005**, *127*, 14190–14191.

(34) Piglosiewicz, I. M.; Beckhaus, R. d.; Wittstock, G.; Saak, W.; Haase, D. *Inorg. Chem.* **2007**, *46*, 7610–7620.

(35) Anderson, J. E.; Gregory, T. P.; McAndrews, C. M.; Kool, L. B. *Organometallics* **1990**, *9*, 1702–1703.

(36) There are two independent molecules of **10** in the unit cell,[31a] with α angles of 2.6° and 1.1°. The α angle of our optimized structure is 1.0°.

(37) Kaim, W.; Reinhardt, R.; Waldhör, E.; Fiedler, J. *J. Organomet. Chem.* **1996**, *524*, 195–202.

(38) Lenges, C. P.; White, P. S.; Marshall, W. J.; Brookhart, M. *Organometallics* **2000**, *19*, 1247–1254.

(39) (a) Kölle, U.; Fuss, B. *Chem. Ber.* **1984**, *117*, 743–752. (b) We note that crystal structures of $[(\eta^5\text{-Cp}^*)\text{M}(\text{bpy}^0)\text{Cl}]^+$ ($\text{M} = \text{Rh}^{\text{III}}, \text{Ir}^{\text{III}}$) have been reported to contain a neutral bpy^0 ligand with a C1—C1′ bond at 1.481(7) and 1.495(5) Å, respectively. Dadci, L.; Elias, H.; Frey, U.; Hörnig, A.; Koelle, U.; Merbach, A. E.; Paulus, H.; Schneider, J. S. *Inorg. Chem.* **1995**, *34*, 306–315.

(40) Mork, B. V.; McMillan, A.; Yuen, H.; Tilley, T. D. *Organometallics* **2004**, *23*, 2855–2859.

(41) (a) Wailes, P. C.; Weigold, H. *J. Organomet. Chem.* **1971**, *28*, 91–95. (b) Beckhaus, R.; Thiele, K.-H. *J. Organomet. Chem.* **1986**, *317*, 23–31. (c) Nitschke, J. R.; Tilley, T. D. *Angew. Chem., Int. Ed.* **2001**, *40*, 2142–2145. (d) Thewalt, U.; Lasser, W. *J. Organomet. Chem.* **1989**, *363*, C12–C14.

(42) (a) Hartl, F.; Rosa, P.; Ricard, L.; Le Floch, P.; Záliš, S. *Coord. Chem. Rev.* **2007**, *251*, 557–576. (b) Stor, G. J.; Stufkens, D. J.; Vernooijs, P.; Baerends, E. J.; Fraanje, J.; Goubitz, K. *Inorg. Chem.* **1995**, *34*, 1588–1594.

(43) (a) Yamaguchi, K.; Takahara, Y.; Fueno, T. In *Applied Quantum Chemistry*; Smith, V. H., Ed.; Reidel: Dordrecht, The Netherlands, 1986;

p 155. (b) Soda, T.; Kitagawa, Y.; Onishi, T.; Takano, Y.; Shigeta, Y.; Nagao, H.; Yoshioka, Y.; Yamaguchi, K. *Chem. Phys. Lett.* **2000**, *319*, 223–230.

(44) Dei, A.; Gatteschi, D. *Inorg. Chim. Acta* **1992**, *198−200*, 813–822.

(45) Albright, T. A.; Burdett, J. K.; Whangbo, M.-H. *Orbital Interactions in Chemistry*; John Wiley & Sons: New York, 1985; Chapter 20.

(46) Two independent molecules are present in the crystal structure of **2**.

(47) Sieger, M.; Kaim, W.; Stufkens, D. J.; Snoeck, T. L.; Stoll, H.; Záliš, S. *Dalton Trans.* **2004**, 3815–3821.

(48) Neese, F. *Orca—an ab initio, DFT and Semiempirical Electronic Structure Package*, version 2.8.0.1, revision 2287; Institut für Physikalische und Theoretische Chemie, Universität Bonn: Bonn, Germany, Dec 2010.

(49) (a) Becke, A. D. *Phys. Rev. B* **1988**, *38*, 3098. (b) Perdew, J. P. *Phys. Rev. B* **1986**, *34*, 7406.

(50) Becke, A. D. *J. Chem. Phys.* **1986**, *84*, 4524–4529.

(51) Becke, A. D. *J. Chem. Phys.* **1993**, *98*, 5648–5652.

(52) Lee, C.; Yang, W.; Parr, R. G. *Phys. Rev. B* **1988**, *37*, 785.

(53) (a) Tao, J.; Perdew, J. P.; Staroverov, V. N.; Scuseria, G. E. *Phys. Rev. Lett.* **2003**, *91*, 146401. (b) Perdew, J. P.; Tao, J.; Staroverov, V. N.; Scuseria, G. E. *J. Chem. Phys.* **2004**, *120*, 6898.

(54) Staroverov, V. N.; Scuseria, G. E.; Tao, J.; Perdew, J. P. *J. Chem. Phys.* **2003**, *119*, 12129.

(55) Schäfer, A.; Horn, H.; Ahlrichs, R. *J. Chem. Phys.* **1992**, *97*, 2571–2577.

(56) Schäfer, A.; Huber, C.; Ahlrichs, R. *J. Chem. Phys.* **1994**, *100*, 5829–5835.

(57) (a) Grimme, S. *J. Comput. Chem.* **2004**, *25*, 1463–1476. (b) Grimme, S. *J. Comput. Chem.* **2006**, *27*, 1787–1799. (c) Grimme, S.; Antony, J.; Ehrlich, S.; Krieg, H. *J. Chem. Phys.* **2010**, *132*, 154104.

(58) Eichkorn, K.; Weigend, F.; Treutler, O.; Ahlrichs, R. *Theor. Chem. Acc.* **1997**, *97*, 119–124.

(59) Eichkorn, K.; Treutler, O.; Öhm, H.; Häser, M.; Ahlrichs, R. *Chem. Phys. Lett.* **1995**, *240*, 283–289.

(60) Eichkorn, K.; Treutler, O.; Öhm, H.; Häser, M.; Ahlrichs, R. *Chem. Phys. Lett.* **1995**, *242*, 652–660.

(61) (a) van Lenthe, E.; Baerends, E. J.; Snijders, J. G. *J. Chem. Phys.* **1994**, *101*, 9783–9792. (b) van Lenthe, E.; Baerends, E. J.; Snijders, J. G. *J. Chem. Phys.* **1993**, *99*, 4597. (c) van Wuellen, C. *J. Chem. Phys.* **1998**, *109*, 392–399.

(62) Pantazis, D. A.; Chen, X. Y.; Landis, C. R.; Neese, F. *J. Chem. Theory Comput.* **2008**, *4*, 908.

(63) Ginsberg, A. P. *J. Am. Chem. Soc.* **1980**, *102*, 111–117.

(64) Noodleman, L.; Peng, C. Y.; Case, D. A.; Mouesca, J. M. *Coord. Chem. Rev.* **1995**, *144*, 199–244.

(65) Kirchner, B.; Wennmohs, F.; Ye, S. F.; Neese, F. *Curr. Opin. Chem. Biol.* **2007**, *11*, 134–141.

(66) Neese, F. *J. Phys. Chem. Solids* **2004**, *65*, 781–785.

(67) Neese, F. *J. Am. Chem. Soc.* **2006**, *128*, 10213–10222.

(68) Molekel, Advanced Interactive 3D Graphics for Molecular Sciences, available under http://www.cscs.ch/molkel/.